CSIRO PUBLISHING

Australian Journal of Physics

Volume 50, 1997

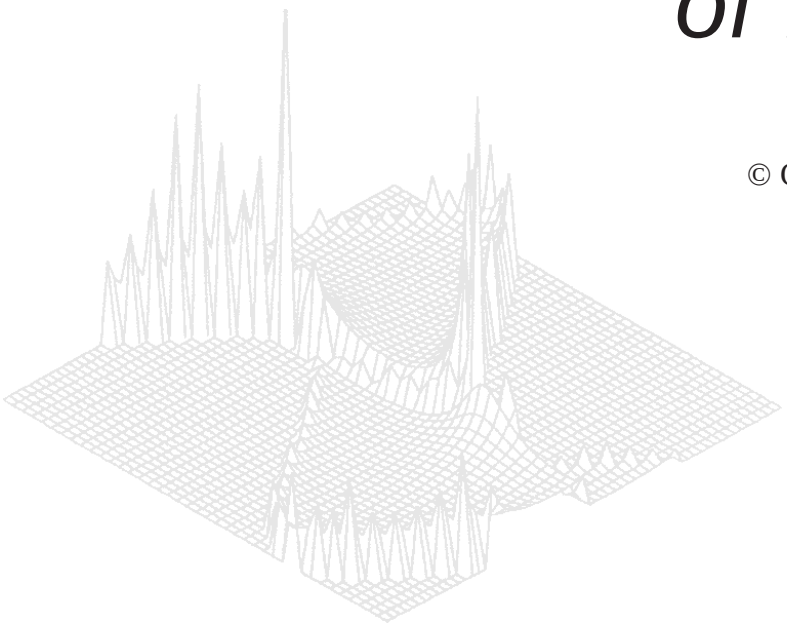

A journal for the publication of
original research in all branches of physics

www.publish.csiro.au/journals/ajp

All enquiries and manuscripts should be directed to
Australian Journal of Physics
CSIRO PUBLISHING
PO Box 1139 (150 Oxford St)
Collingwood Telephone: 61 3 9662 7626
Vic. 3066 Facsimile: 61 3 9662 7611
Australia Email: peter.robertson@publish.csiro.au

Published by **CSIRO** PUBLISHING
for CSIRO Australia and
the Australian Academy of Science

Aust. J. Phys., 1997, **50**, 329–61

Solid State and Magnetic Properties of Pure, Intercalated and Superconducting Fullerenes*

V. Buntar, F. M. Sauerzopf and H. W. Weber

Atominstitut der Österreichischen Universitäten,
Schüttelstr. 115, A-1020 Wien, Austria.

Abstract

A review of some of the solid state and the magnetic properties of fullerenes is presented. We summarise and discuss experimental results on magnetism of pure C_{60}, C_{70} and higher fullerenes. The main features of the structure and the magnetic properties of intercalated fullerenes, such as metallofullerenes, TDAE-C_{60} and polymeric A_1C_{60}, are presented. Attention is also paid to the mixed state properties of fullerene superconductors, especially to the evaluation of the critical fields and the characteristic lengths of these materials. Some new experimental results on this subject are also presented.

1. Introduction

The history of fullerenes started in 1984, when Rohlfing *et al.* [1] and shortly later Kroto *et al.* [2] discovered a new stable form of solid carbon, namely carbon clusters C_n, in addition to the previously known forms, i.e. solid networks, graphite and diamond. The relationship between the crystal structure of graphite, diamond and the C_{60} fullerene as well as their relative binding energies per carbon atom are shown in Fig. 1. In honour of the architect R. Buckminster Fuller this new molecule was called the buckminsterfullerene or fullerene. The latter is now used mainly for the C_{60} molecule, while other C_n clusters are usually called fullerites. Because of the spherical shape of C_{60}, this molecule is sometimes called 'soccerball' or 'buckyball'.

C_{60} consists of 12 pentagons and 20 hexagons, while the nearest neighbour fullerite molecule C_{70} consists of 12 pentagons and 25 hexagons and has a slightly ellipsoidal shape (Fig. 2).

During the first six years after their discovery, fullerenes were considered as exotic materials and investigated mainly theoretically. In 1990 Krätschmer *et al.* [3] discovered a very simple method to extract fullerenes from carbon soot. Since then intensive experimental and theoretical investigations of these materials have started. During this short time they have become one of the most fascinating and rapidly developing areas of modern science.

The materials are indeed interesting for many scientific areas such as chemistry, physics, materials science, biology, and partly 'chemical engineering'. Many

* Refereed paper based on a contribution to the ANZIP 20th Condensed Matter Physics Meeting held at Charles Sturt University, Wagga Wagga, NSW, in February 1996.

10.1071/PH96080 0004-9506/97/020329$15.00

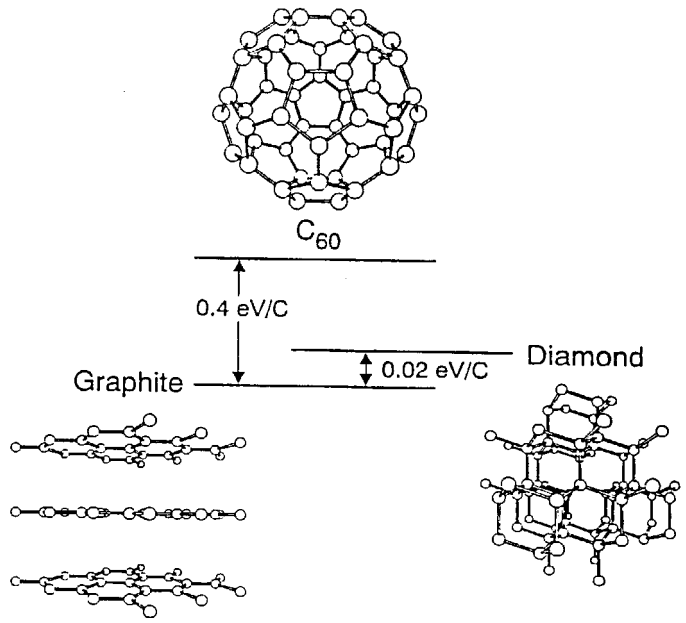

Fig. 1. Relationship between the crystal structures of the three forms of carbon and their relative binding energies per carbon atom. Under normal conditions energy barriers prevent the spontaneous conversion of C_{60} to diamond or graphite. [From Ref. 23]

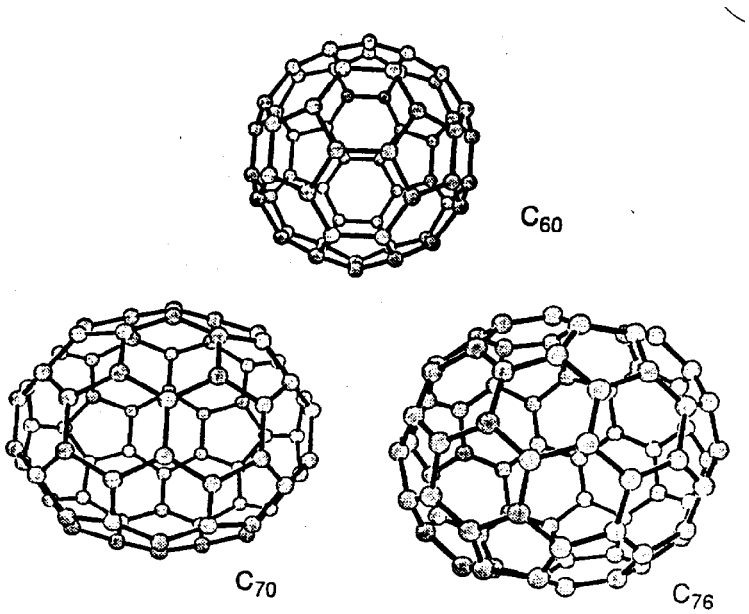

Fig. 2. Molecular structures of three fullerenes isolated in pure form. [After Ref. 16]

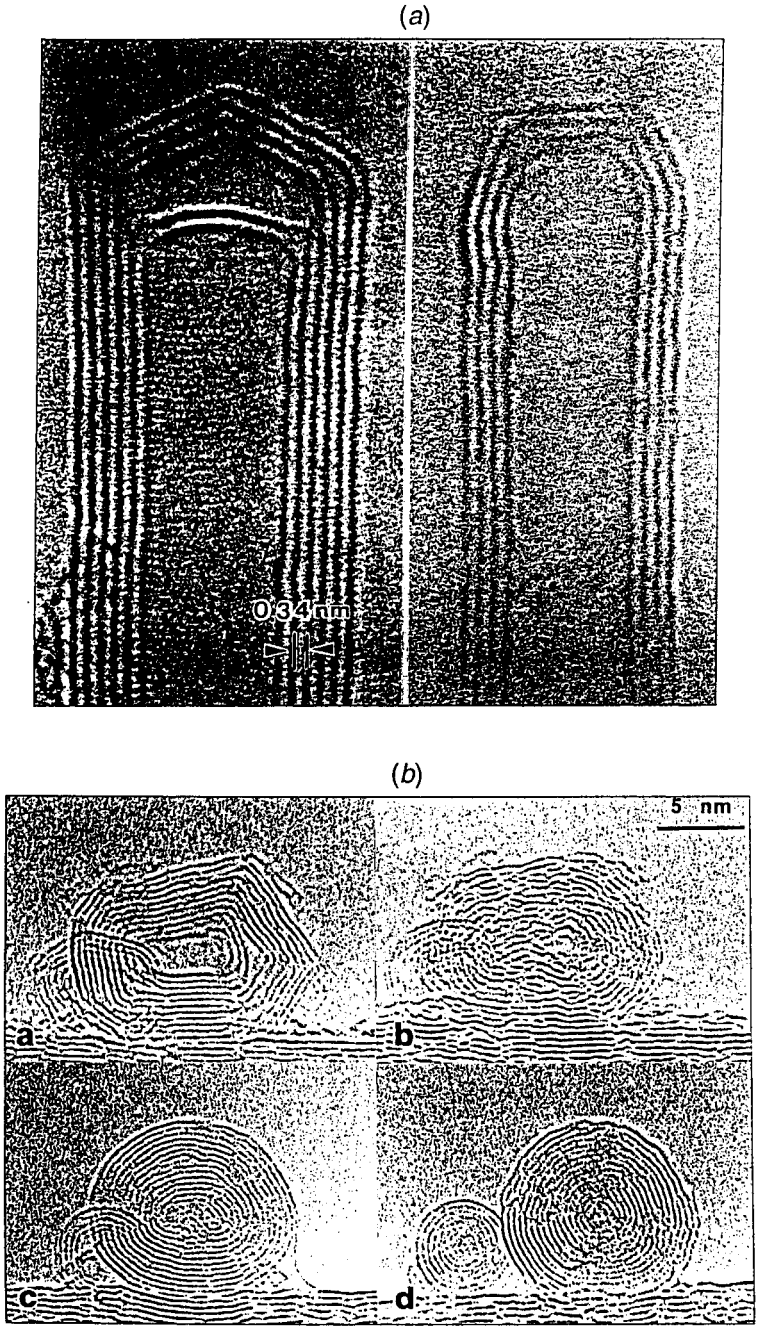

Fig. 3. (*a*) Electron micrographs showing commonly found multi-shell carbon nanotubes. (*b*) Formation of quasi-spherical onionlike particles under electron irradiation: (a) Polyhedral particle as obtained from the electric arc; (b) after 20 s of irradiation the particle collapses and the inner central empty space disappears; (c) after 120 s the reordering begins at the surface and progresses to the centre—at this point we see several closed surface layers and an incompletely formed core; and (d) after 180 s, further irradiation yields a quasi-spherical onion-like particle with a very small central shell. [After Ref. 247]

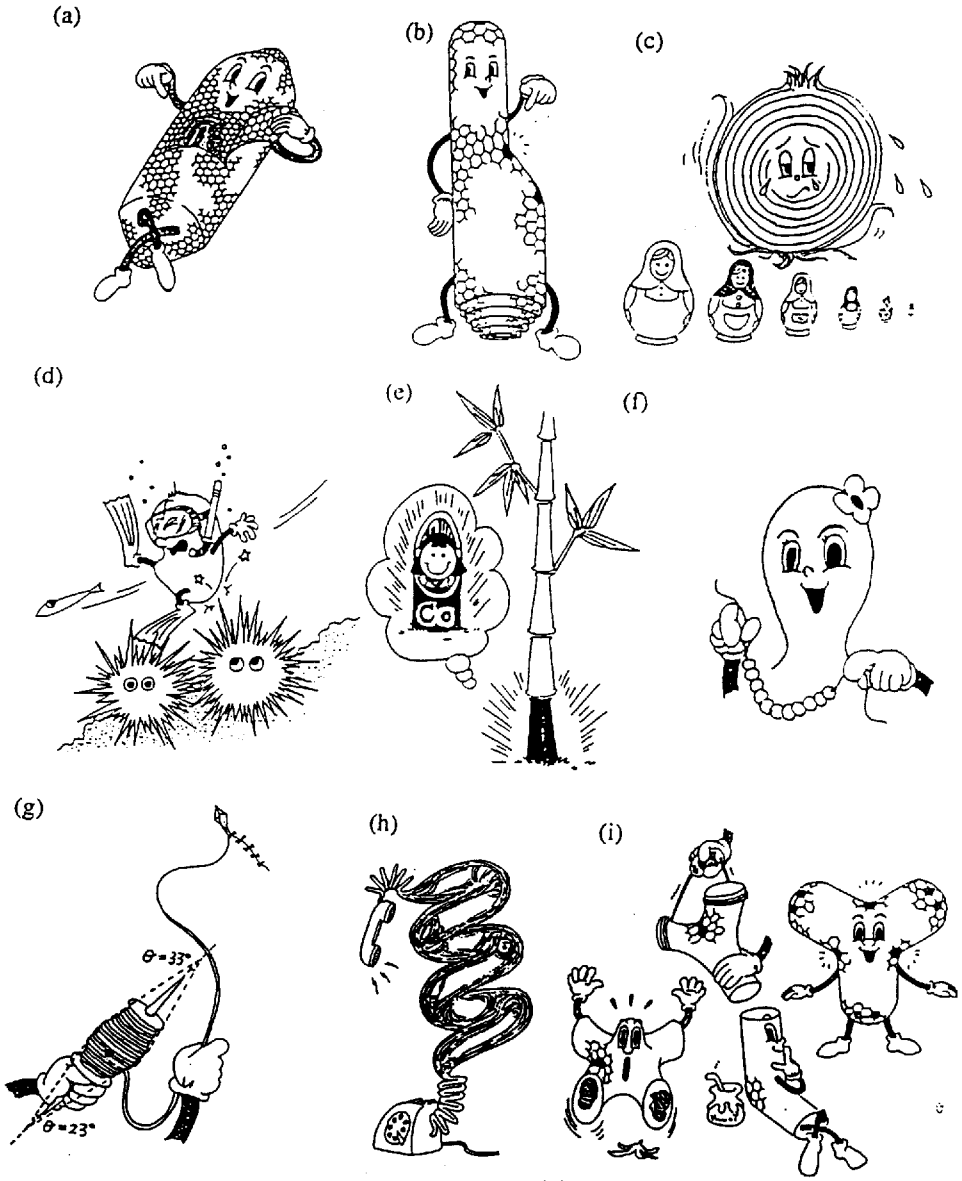

Fig. 4. Illustration of various shapes of fullerenes: (*a*) tube with both ends closed by caps, (*b*) tube with different diameters, (*c*) particle (buckyonions), (*d*) sea urchin, (*e*) bamboo, (*f*) beads, (*g*) spinning cone, (*h*) helical coil, and (*i*) connectors and tripod. [From Ref. 248]

different shapes of fullerenes are observed experimentally, such as carbon sheets, which consist of hexagons only, tubes with open and closed (if pentagons are present in the structure) ends, tubes having different diameters (Fig. 3*a*), buckyonions (Fig. 3*b*), which consist of different fullerites placed inside each other, bamboos, spirals, etc. These shapes are illustrated in Fig. 4.

More than one thousand publications on fullerene physics, chemistry, materials science, biology, etc. have appeared in scientific journals each year since 1990. Special journal issues [4–8] and a special monthly journal, 'Fullerene Science and

Technology', are devoted to this subject. One can find large numbers of books and reviews on the chemical, physical and structural properties of these substances [9–38]. The latter papers overview different subjects of fullerene research. Only one review [38] exists to date, which discusses the magnetic properties of fullerene superconductors. However, because of the large number of experimental results obtained on magnetic properties of different intercalated fullerene compounds, it is worth while, even briefly, to summarise our knowledge of this field.

In this paper an attempt is made to highlight some experimental results on solid state and magnetic properties of fullerenes. We do not discuss all the features in detail, but rather refer the reader after a short discussion to original publications given in the reference section.

This paper is organised as follows. In the next section, we discuss the solid state structure and the magnetism of the undoped C_{60} and C_{70} fullerenes, and higher fullerites. In Section 3, we present the main features of the metallofullerenes, the TDAE-C_{60} derivatives and the polymeric AC_{60} compounds. The section on superconductivity of fullerenes discusses the background of superconductivity in the graphite intercalated compounds and shows results on their normal state properties and their magnetic features in the superconducting state. In Section 5, we present the main experimental results on the critical fields and discuss different methods to obtain the lower critical field of fullerene superconductors. In the last two sections we will discuss flux pinning problems in this type of superconducting materials and address some unsolved questions on the magnetic properties of fullerenes.

2. Solid State Structure of Undoped Fullerenes

Fullerenes are black insulating materials with face centred cubic structure (fcc) at room temperature. The cage diameter of C_{60} is $0 \cdot 71$ nm and the lattice constant is $1 \cdot 42$ nm. The main physical properties of carbon C_{60} are summarised in Table 1.

The magnetism of fullerenes has been of interest since their discovery. The large diamagnetism of graphite suggests that the fullerenes might also display strong π-electron ring currents and an enhanced magnetic susceptibility. Furthermore, if C_{60} is viewed as a sphere with 60 free electrons, which can respond to the application of a magnetic field, the ring current diamagnetism is expected to be 41 times that of benzene [39]. However, despite the trigonal bonding configuration, which is similar to that of graphite, the susceptibiliy χ of C_{60} (Fig. 5) is more than one order of magnitude smaller than that of graphite.

Calculations based on the London theory predicted a vanishingly small π-electron ring current magnetic susceptibility due to the cancellation of the diamagnetism by a very strong Van Vleck paramagnetic term [39, 40]. Experimental results on the magnetic susceptibility of bulk fullerenes confirmed the basic findings of the London calculations [41, 42]. A further treatment shows that the smallness of χ comes from the presence of both five-membered rings (5-MRs) and six-membered rings (6-MRs), which have paramagnetic and diamagnetic ring currents, respectively [43, 44]. The near cancellation of the ring current contributions to χ is due to the unique arrangement of the 5-MRs and the 6-MRs in C_{60}. This is illustrated by considering C_{70}, the susceptibility of which is larger by a factor of 2 than

that of C_{60} despite its structural similarity to C_{60} [41, 42]. Because undoped C_{60} is a semiconductor, there is no contribution to χ from conduction electrons. Thus, χ is a good probe of the intramolecular electronic structure.

Table 1*a*. Properties of solid C_{60} [after Ref. 23]

Property	Value	Reference
Density	$1{\cdot}67\ \mathrm{g\,cm^{-3}}$	[51]
fcc lattice constant	1·4198 nm	[51]
Nearest neighbour distance	1·004 nm	[51]
Bulk modulus	14–18 GPa	[230, 231]
Young's modulus (solvated crystal)	16 GPa	[57]
Vickers hardness	$14{\cdot}5$–$17{\cdot}5\ \mathrm{kg\,mm^{-2}}$	[232]
Volume thermal expansion coefficient	$6{\cdot}2\times10^{-4}\ \mathrm{K^{-1}}$	[233]
Heat of sublimation	140–$160\ \mathrm{KJ\,mole^{-1}}$	[228, 229]
Vapour pressure (500°C)	$6{\cdot}59\times10^{-4}$ mbar	[228]
Thermal conductivity	$0{\cdot}4\ \mathrm{W\ m\,K^{-1}}$	[55]
Debye temperature	74 K	[234]
Refractive index	1·90	[235]
Dielectric constant, static	4·4	[236, 237]
Optical absorption edge	$1{\cdot}5$–$1{\cdot}7$ eV	[237–40]
Transport energy gap	1·9 eV	[241]
Electrical resistivity (300 K)	$\sim10^{14}\ \Omega\,\mathrm{cm}$	[241]
Magnetic susceptibility	$-0{\cdot}35\times10^{-9}\ \mathrm{A\ m^2}$	[41, 42]

Table 1*b*. Properties of the C_{60} molecule [after Ref. 23]

Property	Value	Reference
Cage diameter	0·71 nm	[242]
Intrapentagon C–C distance	0·145 nm	[242]
Interpentagon C–C distance	0·140 nm	[242]
Electron affinity	2·65 eV	[243]
Ionisation potential	7·61 eV	[244]
Binding energy/atom (calculated)	7·0 eV	[245]
Polarisability (calculated)	8·0 nm	[246]

Calculations on high-symmetry giant fullerenes C_n in the size regime $100 < n < 1000$ [45] demonstrate that χ increases monotonically towards the graphite value (Fig. 6). The nanotubes, i.e. higher fullerenes, are also a very interesting subject for magnetic investigations. It was shown [46] from band structure calculations, that the electronic structure of nanotubes is highly sensitive to the degree of helicity of the carbon atom network [47]. Three different categories of helicity are identified, each with its particular band structure. In general, however, the band gap scales with helicity, except for high-symmetry configurations. Because of the interband processes, which lead to the large band

gaps in graphite, it is apparent from the present data that the majority of tubes have a narrow gap band structure similar to that of graphite. DC magnetic experiments [48] showed also an anisotropy of the magnetic susceptibility in carbon nanotubes.

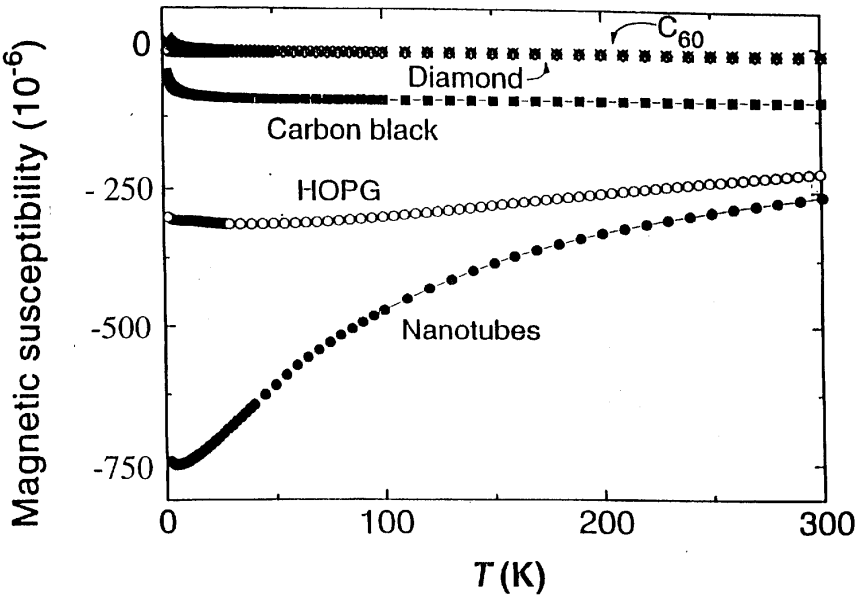

Fig. 5. Orientationally averaged magnetic susceptibility of various forms of carbon. [From Ref. 46]

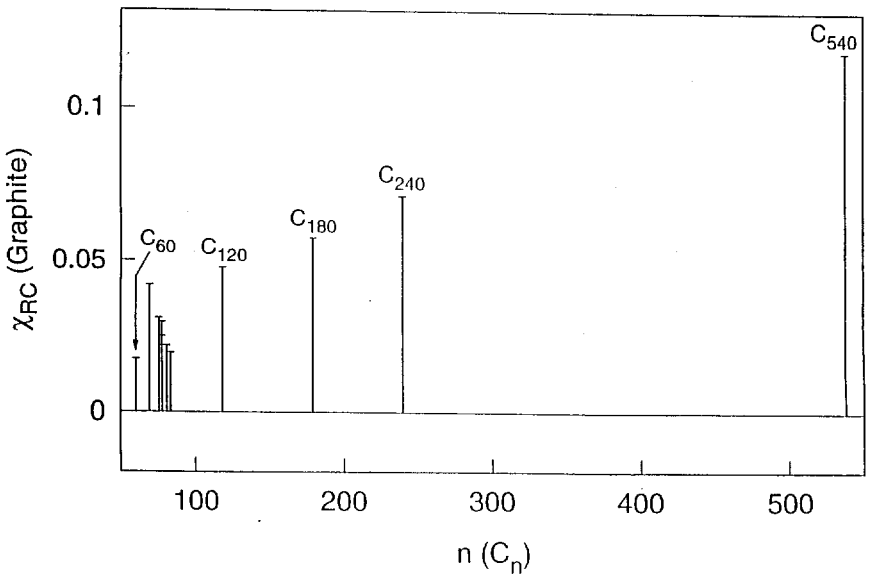

Fig. 6. The π-electron ring current magnetic susceptibilities χ_{RC} as a function of fullerene size $n(\mathrm{C}_n)$, calculated with resonance integrals adjusted for bond strength. [From Ref. 45]

It is well known, that among the fullerenes, the C_{60} molecules have the highest cohesive energy per atom and are the most abundant. This is one of the reasons why the C_{60} fullerene receives primary attention. Having near-spherical shape, these molecules form at low pressures crystal lattices of cubic symmetry. The low temperature phase of the C_{60} fullerene is orientationally ordered and consists of four simple cubic sublattices, which differ from each other by the orientations of the molecules [49, 50]. It is often referred to as the simple cubic (sc) lattice, although it closely resembles the face centred cubic lattice apart from the orientations of its molecules.

Because of their spherical shape, C_{60} molecules can freely rotate in the lattice at high temperatures and the thermal behaviour of solid C_{60} shows several phase transitions due to the orientational re-ordering of C_{60} molecules. At room temperature, solid C_{60} has an fcc crystal structure. The molecules are in complete orientational disorder and form a 'plastic crystal' [49, 51, 52]. With decreasing temperature the system undergoes a first order transition to the sc crystal structure at $T \sim 260$ K [52, 53]. The transition is due to orientational re-ordering, although significant disorder persists to low temperatures [54, 55]. The population of the dominant orientation increases with decreasing temperature down to $T \sim 90$ K, where $83 \cdot 3\%$ of the molecules are in the dominant orientation. This occupancy does not change at lower temperatures [54].

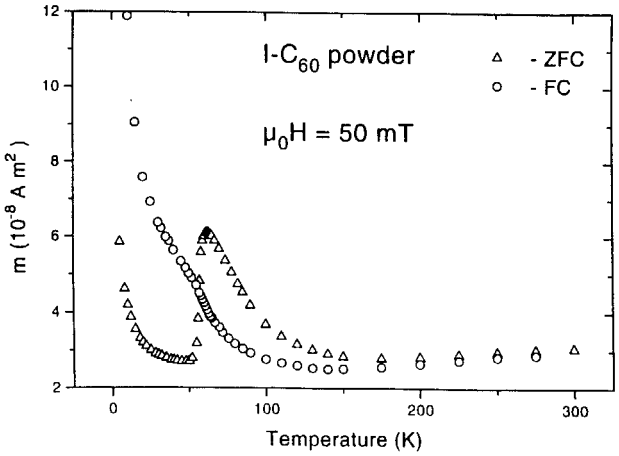

Fig. 7. Temperature dependence of the magnetisation of I_2C_{60} at $\mu_0 H_{\rm ext} = 50$ mT. [From Ref. 62]

At this temperature a glass transition was predicted theoretically [56] and anomalies were observed experimentally by neutron diffraction [54], sound velocity [57], dielectric constant [58], high-resolution dilatometry [59], specific heat [60] and other techniques. Arguments were presented [59–61] that this transition would lead to a frozen glass state. At this temperature, an interesting magnetic behaviour was observed in iodine doped C_{60} [62–65]. Buntar *et al.* [62] performed detailed measurements of C_{60}, C_{70} and I-C_{60} at low temperatures and observed an irreversibility of the magnetisation at $T < 100$ K and a strong extremum at $T \sim 60$ K (Fig. 7). These authors showed that the magnetic phenomena could be due to a transition into a frozen magnetic state.

In the low temperature modification of solid C_{60}, the non-central part of the intermolecular potential leads to orientational ordering of the molecules [66, 67], whereas in the high temperature phase it disappears after averaging over all orientations of the rapidly rotating molecules. Ref. [68] gives a complete set of the thermal and elastic properties in the fcc modification in particular for the high temperature phase.

Unlike the spheroidal C_{60} molecule, the C_{70} molecule has an ellipsoidal shape. This results in an additional degree of freedom for 'packing' the solid and implies that the orientational ordering of the oblong C_{70} solid is much more complex. Vaugham *et al.* [69] reported hexagonal close packed (hcp) and fcc structures for C_{70} crystals. Their X-ray and electron microscopy measurements revealed the presence of more defects than in C_{60}. Fleming *et al.* [70] also reported fcc and monoclinic phases. Verheijen *et al.* [71] found four types of structure: fcc at high temperature, rhombohedral (rh), ideal hcp, and deformed hcp around room temperature. Several groups also reported similar structures [72–75]. It is well accepted now that the thermodynamically stable form of sublimed C_{70} is the cubic close packed one (see for instance Ref. 76).

The rotation dynamics in both the ordered and the disordered phases of C_{70} were studied by a number of experimental techniques such as ^{13}C NMR [77–79], muon spin relaxation [80, 81] and inelastic neutron scattering [82, 83]. At very high temperatures, the orientational motion is described as quasi-isotropic, much like in C_{60}. The first evidence for anisotropy in the motion appears at $T \sim 370$ K, well within the temperature regime of the fcc phase.

3. Intercalated Fullerenes

A large number of chemical elements are considered as intercalants in solid M_xC_{60} compounds or in free $M@C_{60}$ (the symbol @ indicates that the metal atom M is encaged in the fullerene molecule) endothedral complexes or metallofullerenes (see for instance Fig. 2 in Ref. 84). The discovery of C_{60} was soon followed by that of C_{60} with metals encaged, the metal atom being either La or an alkali earth atom [85]. The name 'metallo-fullerenes' has now become common to denote fullerenes with a metal atom inside. The first type of metallofullerene extracted from fullerene soot was lanthanum-fullerene $La@C_{82}$ [86–89] followed a short time later by scandium fullerene $Sc@C_{82}$ [90, 91] and yttrium fullerene $Y@C_{82}$ [90, 92].

Charge transfer to the fullerene units leads to salt or donor–acceptor adduct formation. Intercalation of solid C_{60} with electron donors, like the alkali metals, results in salts with stoichiometries A_xC_{60} with x up to 12 for $Li_{12}C_{60}$. In addition, fullerenes can be intercalated with different organic molecules such as TDAE, tetrakis(dimethyl-amino)ethylene [93], TTF (tetrathiafulvalene) [94], and others.

(3a) Magnetic Fullerene Derivative TDAE-C_{60}

Among the compounds based on C_{60}, the organic molecule TDAE-C_{60} raised quite a lot of interest due to its ferromagnetic-like phase transition at $T = 16$ K (Fig. 8) [93]. Furthermore, the TDAE-C_{60} material has the highest T_c of any molecular organic ferromagnet.

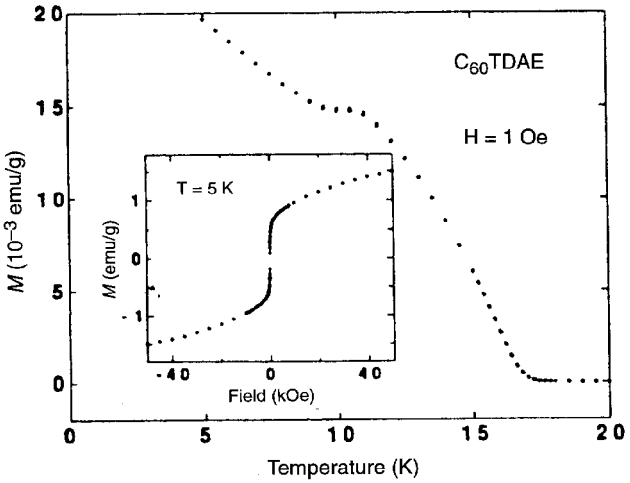

Fig. 8. DC magnetisation as a function of temperature for a pellet of TDAE-C_{60} in an applied field of $0{\cdot}1$ mT. The inset gives the isothermal magnetisation at 5 K. [From Ref. 249]

TDAE is one of the strongest organic donors. In the 1:1 stoichiometry each TDAE molecule donates one electron to the band formed by the lowest unoccupied t_{1u} molecular orbit (LUMO) of the C_{60} units. The crystal is monoclinic [95], with a shorter C_{60}–C_{60} distance along the c axis, and displays 'activated' DC transport properties characteristic of large gap semiconductors [96, 97], or rather a Mott–Hubbard insulator [98].

Several experiments have confirmed by now that TDAE-C_{60} undergoes a soft ferromagnetic spin-glass or superparamagnetic ordering transition below T_c, where the magnetisation versus magnetic field curves become S shaped and strongly nonlinear [93, 99]. Evidence for a magnetic hysteresis curve in TDAE-C_{60} was also reported [100].

The magnetic behaviour is still controversial. Experiments on earlier samples indicated signatures of weak and/or disordered magnetism. Spin glass features were seen in AC susceptibility [101], capacity [102], electron spin resonance (ESR) [103] and muon rotation (μSR) [104] measurements. More recently, long range order was inferred from the rather narrow local magnetic field distribution probed by implanted muons [105, 106], and from single crystal ESR [107]. The strongly anisotropic ESR line intensity was interpreted in terms of an antiferromagnetic exchange along the c axis, leading to weak ferromagnetism of the Dzyaloshinsky–Moria type [108, 109].

Growing experimental evidence points towards a fundamental role played by the orientational (merohedral) order of the Jahn–Teller distorted fullerene molecules for the magnetic properties of this compound. It suggests that the degree of merohedral order, established when the C_{60} orientational degrees of freedom become frozen (at the plastic phase transitions), controls the nature of exchange paths among neighbouring molecules. In particular recent AC susceptibility and ESR measurements [110] show large variations of the magnetic response upon different cooling procedures, from the room temperature plastic phase across the

first freezing temperature of the rotational dynamics of C_{60}. A ten-fold increase of χ'' is observed below T_c for slowly cooled versus quenched samples.

TDAE-higher-fullerite complexes such as TDAE-C_{70}, -C_{84}, -C_{90}, and -C_{96} do not show a ferromagnetic transition, but only paramagnetism at least above $4 \cdot 5$ K [99, 111, 112]. The fact that no magnetic transition was observed in TDAE-C_{70} provides additional evidence that the radical spins reside mainly on the fullerenes. Moreover, the strong narrowing of the ESR line with decreasing temperature together with the observation of relatively high ambient temperature conductivity on a pressed pallet (10^{-2} Ω cm^{-1}) have led to the speculation that TDAE-C_{60} might be metallic and therefore an itinerant ferromagnet [93]. Very recent measurements [96, 113] of the microwave conductivity and optical experiments indicate a clear nonmetallic temperature dependence of the conductivity with a value of the order of 10^{-4} Ω cm^{-1} at 300 K. These authors placed TDAE-C_{60} into the class of semiconducting systems without long-range structural order, where electron localisation eventually leads to a hopping process for electrical transport [96, 113].

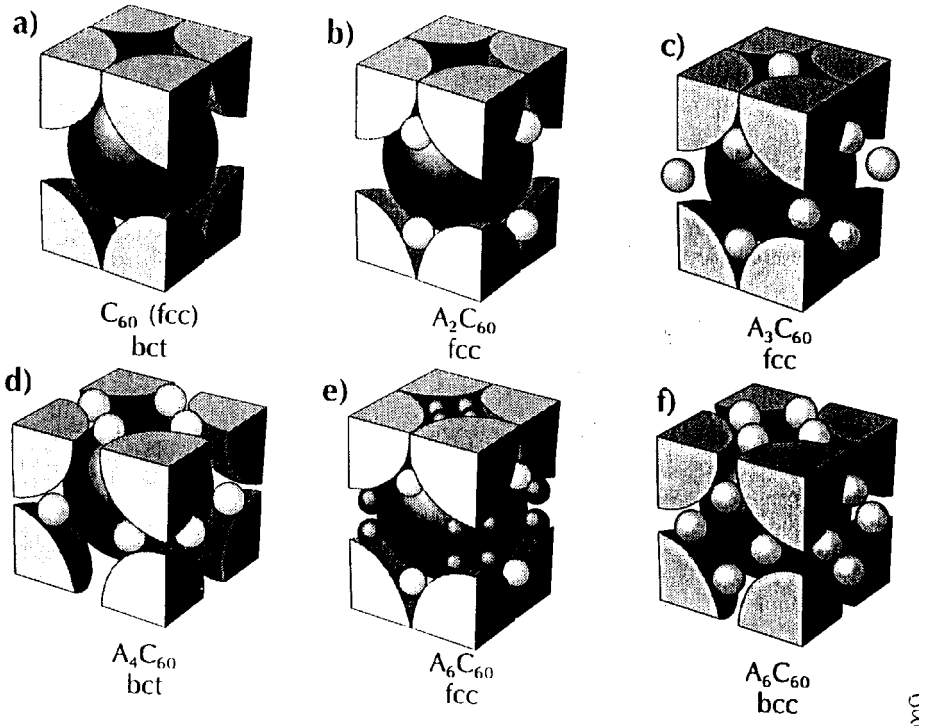

Fig. 9. Structures of C_{60} and A_xC_{60}, where C_{60} is represented by a large sphere and A by a smaller sphere: (*a*) fcc C_{60} drawn in an equivalent bct representation; (*b*) structure of Na_2C_{60} with Na ions in the tetrahedral interstitial sites; (*c*) A_3C_{60} with A ions in both tetrahedral and octahedral interstitial sites; (*d*) A_4C_{60} structure (A = K, Rb and Cs); (*e*) fcc A_6C_{60} structure (A = Na, Ca) with the darker Na 50% occupied; and (*f*) bcc A_6C_{60} structure (A = K, Rb and Cs). [From Ref. 250]

(3b) Alkali Metal Doped Fullerenes

In the beginning, it was believed that only $x = 2$, 3, 4 and 6 stoichiometries are stable for alkali metal doped fullerenes A_xC_{60}. The structures of these compounds are shown schematically in Fig. 9. Shortly after the A_1C_{60} systems were discovered [114], they attracted much interest because of their unusual structural, magnetic and electrical properties. These materials were identified from a Raman analysis of the potassium compound. From X-ray structural investigations the compound was found to have an fcc lattice with a rocksalt structure, where the potassium ions are located on the octahedral interstitial lattice sites [115, 116].

The alkali fullerites AC_{60} (where A = K, Rb and Cs) have a number of stable and metastable modifications. At $T = 370$ K they undergo a first order structural transition from a high temperature fcc to a low temperature orthorhombic phase [117–120]. The structure of this new low temperature phase is quite interesting, since a detailed X-ray investigation [118] resulted in unusually short C_{60}–C_{60} distances along the [110] direction of the original fcc lattice, i.e. only 0·912 nm. This distance implies that the separation between nearest neighbour molecules along the c axis is as small as $\sim$0·2 nm, which has led to the suggestion that the fullerene molecules in this phase polymerise to form an ordered crystalline array of quasi-one-dimensional chains, resembling a lattice of aligned 'necklaces' of fullerene molecules. This polymerisation process is stereochemically similar to the photopolymerisation of C_{60} suggested by Rao *et al.* [121].

For the heavier alkalis (Rb, Cs) this orthorhombic phase undergoes a second electronic phase transition below 50 K. ESR spin susceptibility measurements [117, 122] indicate a magnetic transition at $T \sim 50$ K. The results are shown in Fig. 10. Chauvet *et al.* argued that this was a transition to a spin density wave state. However, detailed electronic structure studies [123, 124] do not support this interpretation. Moreover, several μSR studies [125–28] are consistent with a disordered magnetic phase and not with long range spin density wave order. This magnetic transition is accompanied by a metal–insulator transition [129]. CsC_{60} was found to behave similarly to RbC_{60} in this respect, but KC_{60} was recently claimed to be metallic down to very low temperatures [129].

Metastable phases of monomer C_{60}^- ions or $(C_{60}^-)_2$ dimers were formed by quenching the samples from high temperature to below 300 K [130–33]. Various phase transitions between these phases were reported [134].

Deep quenching of CsC_{60} and RbC_{60} leads to a metallic monomer phase [135], the structure of which was found to be primitive cubic (Pa3) by high resolution powder neutron difraction [136]. This is the only cubic phase of a binary C_{60} salt with a stoichiometry different from A_3C_{60} that is metallic.

4. Superconductivity of Fullerenes

(4a) Background of Fullerene Superconductivity

Superconductivity in graphite intercalation compounds has been known since 1965 when Hannay *et al.* [137] reported transition temperatures in alkali metal graphite intercalation compounds up to 0·55 K for C_8Cs. In the past few years, high pressure synthesis allowed preparation of samples with higher concentrations of alkali metals and resulted in binary graphite intercalated compounds with superconducting transition temperatures as high as 3 K in C_3K and 5 K in C_2Na.

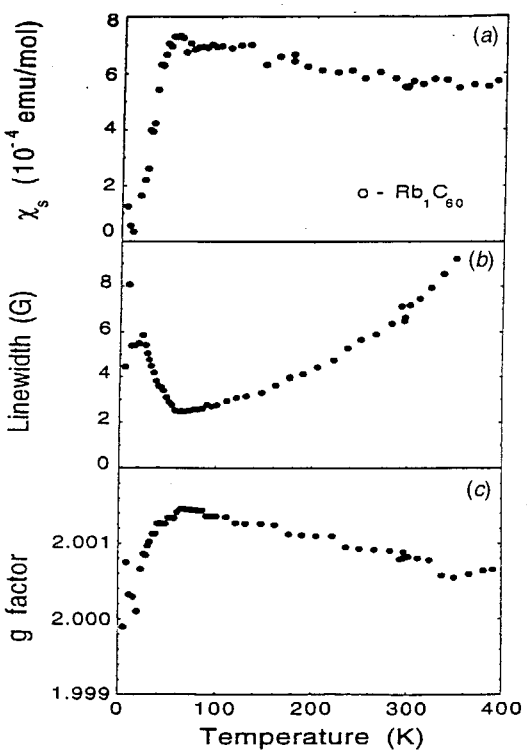

Fig. 10. Magnetic properties of o-RbC_{60}: (a) Above 50 K the spin susceptibility χ_s is large and approximately Pauli-like. (b) The ESR linewidth is narrow despite the structural disorder as expected for a 1D conductor. (c) The broadening and g shift below 60 K is characteristic of a magnetic transition. [From Ref. 117]

Another interesting class of superconducting graphite intercalated compounds, e.g. $C_4KTl_{1\cdot5}$ ($T_c = 2\cdot56$–$2\cdot7$ K), also becomes superconducting as 'second stage compounds' such as $C_8KTl_{1\cdot5}$ ($T_c = 1\cdot3$–$2\cdot45$ K).

Conductivity [138] and superconductivity [139, 140] of the alkali-metal doped fullerenes were discovered less than one year after the production method for bulk quantities of C_{60} and C_{70} had been published [3]. The phenomenon of superconductivity is one of the most fascinating properties of 'the roundest of all round molecules' [11], which attracted enormous scientific interest in this new form of carbon. In many aspects the situation was similar to that shortly after the discovery of superconductivity at high temperatures in the copper oxides [141, 142]. Fullerene superconductors were the second group of materials besides the cuprates, which overcame the previous boundary for the critical temperature, $T_c = 23\cdot2$ K (Nb_3Ge), in conventional superconductors. More than twenty superconducting compounds of doped fullerenes have been synthesised by now. The highest critical temperature ($T_c = 33$ K) occurs in the fullerene $RbCs_2C_{60}$ [143]. (Palstra *et al.* [144] reported superconductivity in Cs_3C_{60} with $T_c = 40$ K at high pressure; however, this result has not yet been reproduced.) These new superconducting compounds can be prepared easily by heating alkali metal–C_{60} mixtures at $T \sim 300$°C or by keeping C_{60} in an alkali metal vapour atmosphere. However, to get from the synthesis of individual samples to practical applications of these superconductors, numerous investigations of the physical properties, stability, reproducibility, and the elaboration of technologies for the production of large quantities for technical use are required. One of the biggest

problems is their instability against air. It is enough to expose the material to air for a fraction of a second to completely destroy superconductivity.

Numerous experimental investigations of these superconductors, both in granular and in crystalline form, show unique properties and distinguish them from other superconducting materials. It was shown (see for instance Ref. 145) that superconductivity in alkali metal doped fullerenes occurs in the face centred cubic (fcc) crystal phase with the composition $A_xB_{3-x}C_{60}$ [146]. Other crystalline phases, such as body centred cubic (bcc) and body centred tetragonal (bct), do not show superconductivity. In the other family of fullerene superconductors, i.e. alkali-earth-doped C_{60}, superconductivity occurs in simple cubic Ca_5C_{60} [147] and in bcc Sr_6C_{60} [145] and Ba_6C_{60} [148]. (An additional phase, possibly Ba_4C_{60}, was found from X-ray diffractometry and there is some evidence [149] that this phase could be responsible for the occurrence of superconductivity in Ba compounds.) Intercalation of fullerites with rare-earth (RE) metals Yb, Sm and Eu has led to superconductivity in $RE_{2\cdot75}C_{60}$ compounds with $T_c \sim 6\,\mathrm{K}$ [150]. Furthermore, a superconducting phase in the lanthanum fullerite La_xC_{60} was found from microwave absorption measurements below $12\cdot5\,\mathrm{K}$ [150].

New silicon clathrate compounds containing barium with an alkali metal, $(Ba,\ A)_xSi_{46}$ (A = Na, K), have recently been synthesised and reported to be superconducting [151–54]. The barium containing clathrate compounds as well as the C_{60} based ones are type-II superconductors with a T_c of about 4 K. Diamagnetism due to superconductivity was observed [151] in good agreement with resistivity measurements. Chemical analysis showed that the compositions of the clathrates were close to the ideal composition of $Ba_6A_2Si_{46}$. The silicon clathrate compound consists of a Si-sp3 open network having two types of cages, Si_{20} pentagonal dodecahedra and Si_{24} tetrakaidecahedra, the two types of polyhedra being linked by shared faces. The X-ray Rietveld analysis shows that the alkali metal atoms mainly occupy the former and the barium atoms the latter cages. This is the first superconductor found for a Si-sp3 covalent network.

One of the most important results is the experimentally established empirical linear correlation of the transition temperature T_c both with the lattice constant of the cubic structure a [143, 146, 155, 156] and with the density of states at the Fermi level [157–59]. Transition temperatures of different A_xC_{60} superconductors versus the fcc lattice parameter a are shown in Fig. 11. This relationship also holds for the corresponding alloys as well as for these materials under lattice compression [160, 161] (Fig. 12). The slope of this linear $T_c(a)$ relation depends on the structural type [162–64]. Very recently [165], a second much steeper $T_c(a)$ dependence was found for the space group Pa [166], which could lead to much higher T_c values if only a slight increase in a could be achieved (see Fig. 13). Fig. 13 also shows a difference between ambient (solid line) and high pressure (dotted line) data, in contrast to the case of the fcc superconductors where both sets of data coincide.

(4b) Normal State Properties

Doping C_{60} with alkali metals leads to a change of its electrical resistivity from very high values (10^8–10^{10} Ω cm for C_{60}) to a metallic-like behaviour in A_xC_{60}, because the doping results in a charge transfer to the C_{60} molecules and strongly increases the π–π overlap between them, enhancing the electrical

conductivity. The electrical resistivity ρ approaches a minimum at $x = 3$, where it reaches typical values of high resistivity metals [167, 168]. The low electrical conductivity can be explained by the relatively weak overlap of the electron wavefunctions between the adjacent C_{60}^{3-} ions and by the merohedral disorder in the alignment of adjacent C_{60}^{3-} ions.

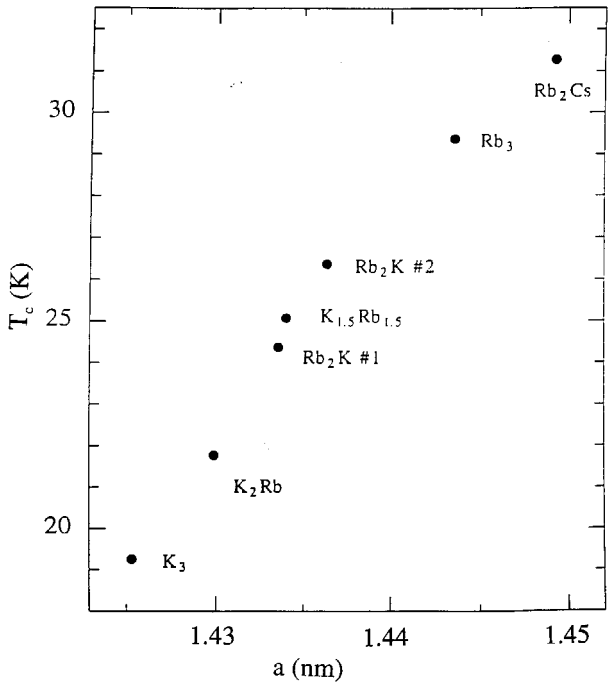

Fig. 11. Variation of the superconducting transition temperature T_c with fcc lattice parameter a for various compositions of A_3C_{60}. [From Ref. 155]

Xiang *et al.* [169] measured the resistivity of single crystal K_3C_{60} and obtained a metallic behaviour $\rho(T)$ between 20 and 300 K, with a residual resistivity of $2{\cdot}5$ mΩ cm. Hebard *et al.* [170] reported measurements of the resistivity $\rho(T)$ for both K_3C_{60} and Rb_3C_{60} thin films. The results revealed a metallic behaviour up to 520 K without any evidence for saturation and a linear temperature dependence of the resistivity above 300 K. For Rb_3C_{60} they found that the residual resistivity was about $1{\cdot}1$ mΩ cm, which is less than that reported in Ref. [169]. Based on a spherical Fermi surface and on the traditional Bloch–Boltzmann approximation, the authors obtained the transport scattering length $l_{\mathrm{tr}} = 0{\cdot}063$ nm calculated from $\rho(520\ \mathrm{K}) = 5{\cdot}5$ mΩ cm, which is significantly shorter than the nearest neighbour distance between the C_{60} molecules (1 nm) and the average separation of $0{\cdot}6$ nm between the conduction electrons, and even shorter than the distance between neighbouring C atoms in each C_{60} molecule ($0{\cdot}14$ nm). Even for the residual resistivity ($1{\cdot}1$ mΩ cm) we still get $l_{\mathrm{tr}} = 0{\cdot}3$ nm, which is too short. All this seems to indicate that the electron is for the most part confined within the surface of a given molecule before hopping to the next one. In addition, the transport electron–phonon coupling constant λ_{tr} was estimated in Ref. [170] and

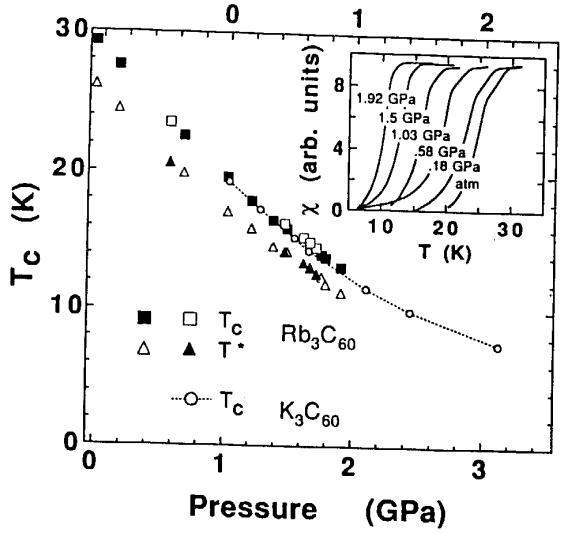

Fig. 12. The inset shows the temperature dependence of the magnetic susceptibility of polycrystalline pressed pellets of Rb_3C_{60} at various pressures. The lower transition T^* is indicative of an intergranular coherence transition. The bulk superconducting transition T_c is determined as the point of highest curvature. The pressure dependence of T_c is shown for both K_3C_{60} and Rb_3C_{60}. The solid and open symbols correspond to data taken under increasing and decreasing pressure, respectively. The K_3C_{60} data have been shifted by $1{\cdot}06$ GPa, and the two data sets have the same pressure dependence $T_c(P) = T_c(0)\exp(-\gamma P)$, where $\gamma = 0{\cdot}44 \pm 0{\cdot}03$ GPa^{-1}. [From Ref. 249]

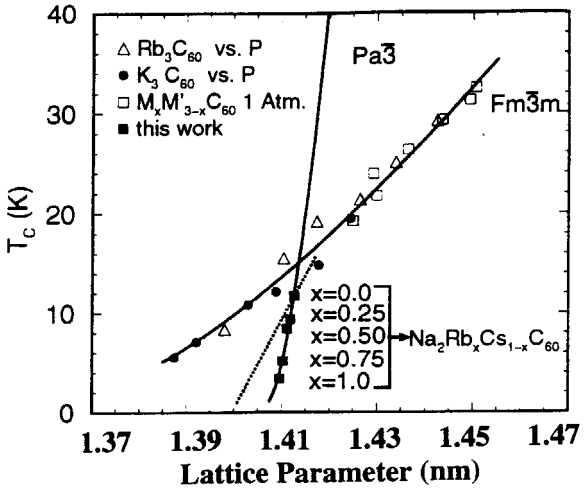

Fig. 13. Plot of T_c versus a for Fm3m [143, 156] and Pa3-ordered superconductors [166]. Solid and dashed lines are fits to McMillan's formula using linear and power law dependencies, respectively, of $N(E_F)$ on the intermolecular distance; only the parameters describing $N(E_F)$ versus a differ in the fits for the two families of materials. The slope of the Pa3 curve is much larger than that for Fm3m, indicating that a small increase of a without destroying Pa3 ordering should cause T_c to increase very rapidly. The dotted line represents the results of Ref. [251]. [After Ref. 166]

found to be $\lambda_{tr} = 4 \cdot 4$ for Rb_3C_{60}, i.e. clearly strong coupling. Both of these results, a short λ_{tr} and strong electron–phonon coupling, indicate predominant intramolecular electron–phonon interaction.

Vareka *et al.* [171] found that under conditions of constant sample volume the normal state resistivity of Rb_3C_{60} has a linear temperature dependence, $\rho \sim T$, in sharp contrast to $\rho \sim T^2$ observed under conditions of constant sample pressure. This result is important because positive $\delta\rho(T)/\delta T$ is consistent with metallic behaviour and the linear term in the temperature dependence of $\rho(T)$ is consistent with an electron–phonon scattering mechanism.

Measurements of the magnetic susceptibility χ in the normal state by Ramirez *et al.* [158] and by Wong *et al.* [172] demonstrated that the susceptibility was positive. The susceptibility $\chi(T)$ was found to be temperature independent, consistent with the metallic Pauli susceptibility.

More results and discussions of the normal state scattering mechanisms can be found in Refs [33, 34, 173–78].

(4c) Magnetisation Curves

The first experiments on K_3C_{60} [179] and Rb_3C_{60} [180, 161] established that alkali doped fullerenes were 'strong' type-II superconductors and that their main superconducting parameters, the Ginzburg–Landau parameter κ, the penetration depth λ, the coherence length ξ, and the critical fields H_{c1} and H_{c2}, were very similar to those of the high-T_c oxides.

Typical temperature and magnetic field dependencies as well as the time relaxation of the magnetisation M, measured on K_3C_{60} and Rb_3C_{60} superconductors [180, 181] with a SQUID magnetometer, are shown in Figs 14, 15 and 16 [182]. We wish to point out, that the ZFC magnetisation shows the flux exclusion from the sample, while the FC magnetisation shows the flux expulsion. A big difference between zero-field-cooled (ZFC) and field-cooled (FC) curves (Fig. 14) and a strong hysteresis in the magnetic field dependence of the magnetisation at fixed temperature (Fig. 15) indicate pinning of the magnetic vortices. The fact that the FC signal of the K_3C_{60} crystal (Fig. 14) is very small and lies close to the zero-magnetisation line shows that pinning in the sample is extremely strong and that there is almost no expulsion of the magnetic field.

The magnitudes of the ZFC and FC magnetisation at the lowest temperature can be used for an evaluation of the 'superconducting fraction' X_{sc}. The fraction can also be evaluated from the slope of the linear dependence of M on H at $H < H_{c1}$. The latter method was used in Refs [183, 184] and appears to be better than the former.

Detailed discussions of these evaluations can be found in Ref. [38], where we pointed out that a quantitative evaluation of X_{sc} is difficult, especially for powdered samples, and should be done very carefully. Almost all of the superconducting volume fractions published for fullerene superconductors were obtained from ZFC measurements and vary between 40 and 90% in powder samples [146, 148, 185–88]. We believe that these values should be treated as a lower limit because of granularity effects [189, 190].

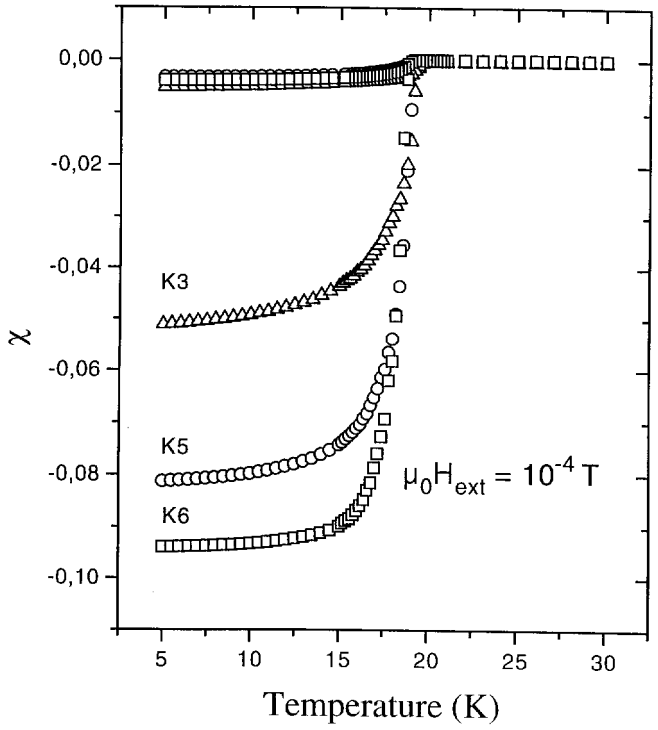

Fig. 14. Temperature dependence of the zero-field cooled (ZFC) and field-cooled (FC) d.c. magnetic susceptibility of K_3C_{60} crystals with 65% superconducting fraction (K3) and 100% superconducting fraction (K5 and K6). The difference in the absolute value of χ for K5 and K6 is due to the influence of the geometrical demagnetisation factor. [From Ref. 203]

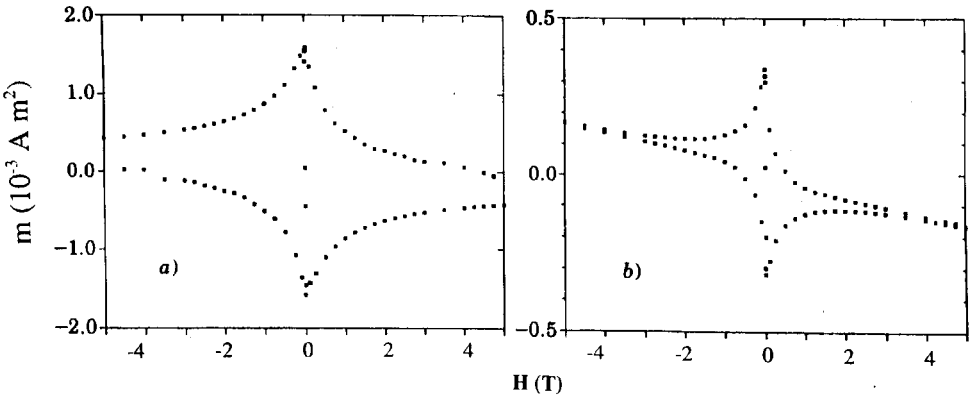

Fig. 15. Hysteresis loops for Rb_3C_{60} powder at (*a*) $T = 7$ K and (*b*) $T = 20$ K. [From Ref. 180]

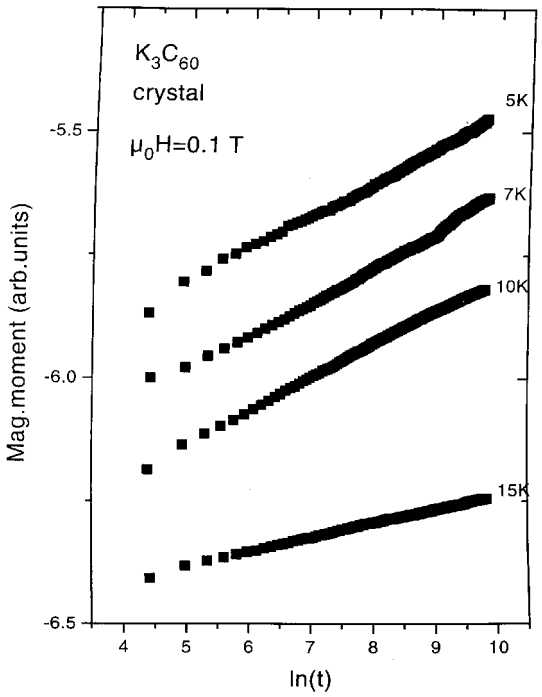

Fig. 16. Time dependent magnetisation in an external magnetic field $\mu_0 H_{\text{ext}} = 0{\cdot}1$ T at 5, 7, 10 and 15 K. [From Ref. 182]

5. Critical Fields and Characteristic Lengths of Fullerene Superconductors

(5a) Upper Critical Field and Coherence Length

A large number of experiments was made to determine the upper critical field for crystalline [169, 175, 181, 191–93] and powdered [159, 161, 179, 180, 183–85, 190, 194–98] fullerenes as well as for thin films [176] using different techniques such as magnetisation [161, 179, 180, 184, 198], ac-susceptibility [190, 195], transport [176, 197], rf-absorption [196], etc. Almost all measurements were done on K_3C_{60} and Rb_3C_{60} and only a few results are available on each of $RbCs_2C_{60}$ [184], K_2CsC_{60} and Rb_2CsC_{60} [199] and Ba_6C_{60} [200]. Other superconducting fullerenes have not yet been characterised.

Typical results on the temperature dependence of the upper critical field are shown in Fig. 17. Measurements of H_{c2} are limited by the experimentally achievable magnetic fields, which are usually not larger than 5–8 T. The extrapolation of $H_{c2}(T)$ to zero is subject to a large uncertainty and depends on the fitting scheme. The standard theory by Werthamer–Helfand–Hohenberg (WHH) [201] is usually employed. This theory predicts an $H_{c2}(T)$ dependence, which follows roughly a power law $h = 0{\cdot}6\ (1{-}t^{\alpha})$, where $t = T/T_c$, $h = H/H_{c2}$ and $\alpha \approx 1{\cdot}75$. Here $H_{c2}(0)$ can be evaluated from the slope, H'_{c2} near T_c. In order to verify the applicability of this relation to C_{60}-based materials, several experiments were performed up to very high magnetic fields [194–96]. Good agreement of the experimental data with the WHH prediction was obtained [194–96] demonstrating that this theory is successful in describing fullerene superconductors (Fig. 18).

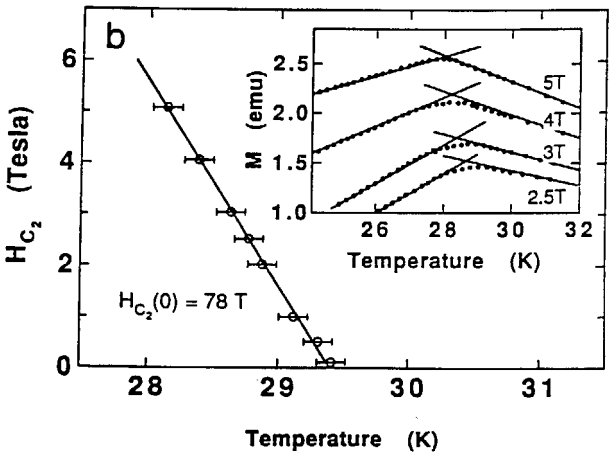

Fig. 17. Temperature dependence of the upper critical field H_{c2}. The inset indicates the method for determining T_c from magnetisation data at different magnetic fields. [From Ref. 161]

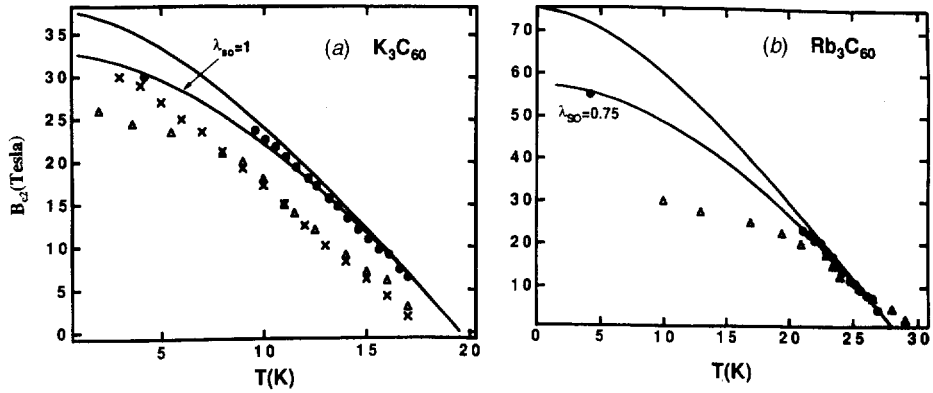

Fig. 18. Upper critical field versus temperature for (*a*) K_3C_{60} powder and (*b*) Rb_3C_{60} powder. The low field data are taken in d.c. fields and the data points at 4·2 K are taken in pulsed fields. The lower solid curves are fits to the data (•) including Pauli paramagnetic limiting and the upper curves assume no paramagnetic limiting. Both experimental dependencies follow roughly the WHH prediction [201]. [After Ref. 196]

From $H_{c2}(0)$, the coherence length ξ can be calculated using the Ginzburg–Landau relation [202]

$$\mu_0 H_{c2} = \frac{\Phi_0}{2\pi\xi^2}, \tag{1}$$

with $\Phi_0 = h/2e = 2\times10^{-15}$ Wb, where Φ_0 is the flux quantum, h is Planck's constant and e is the electron charge. The coherence length of fullerene superconductors is very small (a few nanometres) and comparable to the short ξ of high-T_c superconductors. According to Ref. [198] the temperature dependence of the coherence length and the penetration depth in Rb_3C_{60} can be well described

by Ginzburg–Landau theory in the temperature range $0{\cdot}85 < T/T_c < 1$.

A strong scatter of the experimental data is found for $H_{c2}(0)$ and H'_{c2} (Table 2). For example, for K_3C_{60} H'_{c2} varies from -2 to $-5{\cdot}5\,\mathrm{T\,K^{-1}}$ and for Rb_3C_{60} from -2 to $-3{\cdot}9\,\mathrm{T\,K^{-1}}$. Very recently Buntar *et al.* [203] performed detailed magnetic measurements of the upper critical field on a bulk K_3C_{60} crystalline sample of a good quality. The temperature dependence of H_{c2} obtained in this work is shown in Fig. 19. Here $H_{c2}(\mathrm{T})$ is linear at these temperatures with a slope $H'_{c2} = -2{\cdot}1\,\mathrm{T\,K^{-1}}$, which leads to $\mu_0 H_{c2}(0) = 28\,\mathrm{T}$ and $\xi(0) = 3{\cdot}4\,\mathrm{nm}$.

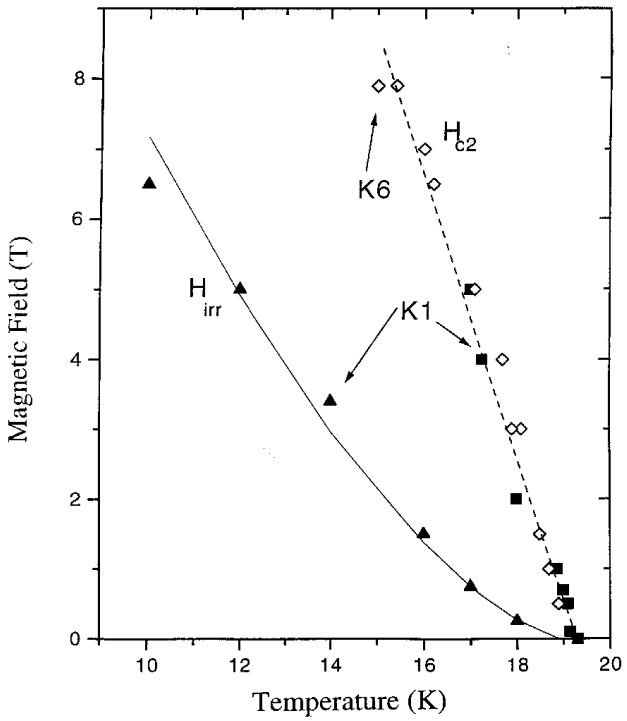

Fig. 19. Temperature dependence of the upper critical field for a sample with 25% superconducting fraction (K1—solid squares) and with 100% superconducting fraction (K6—open diamonds) and of the irreversibility line (solid triangles) for K1. [From Ref. 203]

(5b) Lower Critical Field and Penetration Depth

The first results on H_{c1} for K_3C_{60} [179], Rb_3C_{60} [180, 161], $RbCs_2C_{60}$ [184] and Ba_6C_{60} [200] were obtained by a dc-magnetisation technique. The $H_{c1}(0)$ evaluated from these measurements lies in the range $\mu_0 H_{c1} = 10$–$16\,\mathrm{mT}$ (see Table 2). The temperature dependence of H_{c1} can be described well by $H_{c1}(T)/H_{c1}(0) = 1-(T/T_c)^2$ [179] and an example of this dependence [204] is shown in Fig. 21 below. From $H_{c1}(0)$, the penetration depth λ is evaluated using the well known equation

$$\mu_0\, H_{c1} = \frac{\Phi_0}{2\pi\lambda^2} \ln\kappa \tag{2}$$

and the value of the coherence length known from independent measurements (Section 5*a*). The magnitude of λ obtained in this way is of the order of 200–250 nm (Table 2).

Table 2*a*. Experimentally obtained mixed state parameters of fullerene superconductors [after Ref. 215]

Compound	T_c (K)	$H_{c1}(0)$ (mT)	$H_{c2}(0)$ (T)	$-H'_{c2}$ (T K^{-1})	λ (nm)	ξ (nm)	χ
K_3C_{60}	18·5 [195]	13·2 [179]	17 [190]	1·4 [190]	240 [172]	2 [172]	92 [179]
	19 [216]	4·2 [211]	17·5 [191]	1·34 [191]	240 [179]	2·6 [179]	53 [191]
	19·3 [155]	1·2 [181]	28 [203, 194]	2 [181, 194]	240 [191]	2·9–3·3 [195]	262 [181]
	19·5 [196]		30–38 [195]	2·14 [195]	480 [212]	3·4 [181, 194]	
	19·7 [191]		38 [196]	2·18–2·8 [197]	480 [213]	4·4 [190]	
			47 [176]	2·8 [196]	600 [218]	4·5 [191]	
			49 [179]	3·5 [158]	800 [219]		
				3·73 [179]	890 [181]		
				5·5 [176]			
Rb_3C_{60}	27·5 [180]	9–11·4 [183]	40 [194]	2 [194]	320 [192]	2 [161]	80·5 [204]
	28 [140]	12 [161]	44 [183]	2·5 [183]	240–280 [183]	2·3 [183]	104–122 [183]
	29 [143, 220]	16·2 [204]	44 [190]	2·3 [190]	215 [204]	2·4 [192]	123 [161]
	29·4 [155]	3·2 [211]	46·5 [180, 221]	2·2 [221]	247 [161]	2·7 [180, 190]	315 [181]
	30 [192]	1·3 [181]	62 [192]	3·28 [192]	420 [213]	3 [194]	
			76 [196]	3·86 [196]	460 [218]		
			78 [161]	3·9 [161]	530 [222]		
					800 [219]		
					850 [181]		
$RbCs_2C_{60}$	33 [145, 184]	81 [184]	0·8 [184]	17 [184]	300 [184]	4·4 [184]	68 [184]
Ba_6C_{60}	7 [148, 200]	13 [200]	0·45 [200]	2·2 [200]	180 [200]	12 [200]	15 [200]

Table 2*b*. Experimentally obtained superconducting parameters of fullerenes after Ref. [215]

Compound	J_c (A m^{-2})	$2\Delta/k_B T_c$	Activation energy (meV)
K_3C_{60}	10^9 [190]	3·4 [172]	33–55 [182]
	$1·2\times10^9$ [179]	1·76 [212]	10–60 [223]
	10^9 [210]	3·52 [179]	
	10^7 [211]	5·2 [224]	
Rb_3C_{60}	10^9 [190]	3–4 [224]	33 [180]
	$1·5\times10^{10}$ [161]	4·1 [193]	
	2×10^{10} [198]	5·08 [225]	
	4×10^{10} [180]	7·7 [226]	
	$\sim10^{10}$ [210]	5·4 [227]	
	$\sim10^7$ [211]		

In these experiments the lower critical field was defined as the field at which a deviation from linearity in $M(H)$ first appeared. Indeed, an ideal superconductor exhibits linear $M(H)$ behaviour up to H_{c1}, where a sharp cusp occurs. However, none of the magnetisation data for fullerene materials show good linearity or any cusps (Fig. 20). (The nature of such a behaviour is discussed in Ref. 32.) Usually $M(H)$ has a smooth positive (Fig. 20*a*) (in some experiments even a negative—see Fig. 20*b*) curvature. It is extremely difficult to obtain the point of first deviation from such a curve, since the deviations themselves are very small.

In order to make this procedure more quantitative, it is tempting to apply Bean's critical state model [205] for the entry of vortices into hysteretic superconductors. According to this theory, a plot of δM versus H^2, where $\delta M = M + H_a$ is the deviation of the observed magnetisation from perfect diamagnetic behaviour, should give the lower critical field. This analysis was done for Rb_3C_{60} [204] and $RbCs_2C_{60}$ [184]. In Ref. [184] these data agreed well with the data obtained from the first deviation from a linear dependence. However, both methods led to extremely high values of H_{c1} at low temperatures and did not provide us with the 'intrinsic' values of the lower critical field. In Ref. [204], the data obtained from Bean's analysis showed much smaller values of H_{c1} (triangles in Fig. 21) and the authors related their data to the field at which breaking of intergranular Josephson junctions occurs.

The two methods above obviously do not lead to satisfactory results. Therefore, Politis *et al.* [183] and Buntar *et al.* [184] used an analysis, which is based on measurements of the reversible magnetisation at high external fields, and calculated H_{c1} from the well known Ginzburg–Landau relations [206]:

$$-M = \frac{H_{c2}(T) - H}{(2\kappa^2 - 1)\beta_a}; \qquad -M = \frac{\alpha\Phi_0}{8\pi\mu_0\,\lambda^2(T)} \ln\frac{\beta H_{c2}(T)}{H} \tag{3}$$

for high and intermediate magnetic fields, respectively. This analysis led to lower critical fields, which were slightly smaller but comparable to the data obtained by the first two methods [183, 184].

The last method, based on direct measurements of the reversible magnetisation at high temperatures, is more accurate for the determination of the lower critical field. However, the resulting values of the Ginzburg–Landau parameter κ and, hence, of H_{c1} strongly depend on the value of the superconducting fraction assumed [see Ref. 184, equation (4)]. This leads to an enormous uncertainty in quantitative calculations, especially in the case of powdered samples with a large distribution of grain sizes.

In order to avoid the difficulties associated with the previous three methods, another way to evaluate H_{c1} must be found. In our recent investigations we used a method developed by Böhmer [207], in which H_{c1} is determined through measurements of the trapped magnetisation. This method is far more accurate than the measurements of δM because of the cancellation of a large linear contribution [208]. It is based on the fact that trapped magnetic flux, M_t, can be built up in a sample only when the field had been increased beyond H_{c1}. The advantage of this method for type-II superconductors with strong pinning was illustrated in Ref. [208], where the $M(H)$ behaviour was shown to appear quite linear in the vicinity of H_{c1}, whereas ${M_t}^{1/2}$ versus H showed a well resolved kink at the field corresponding to H_{c1}.

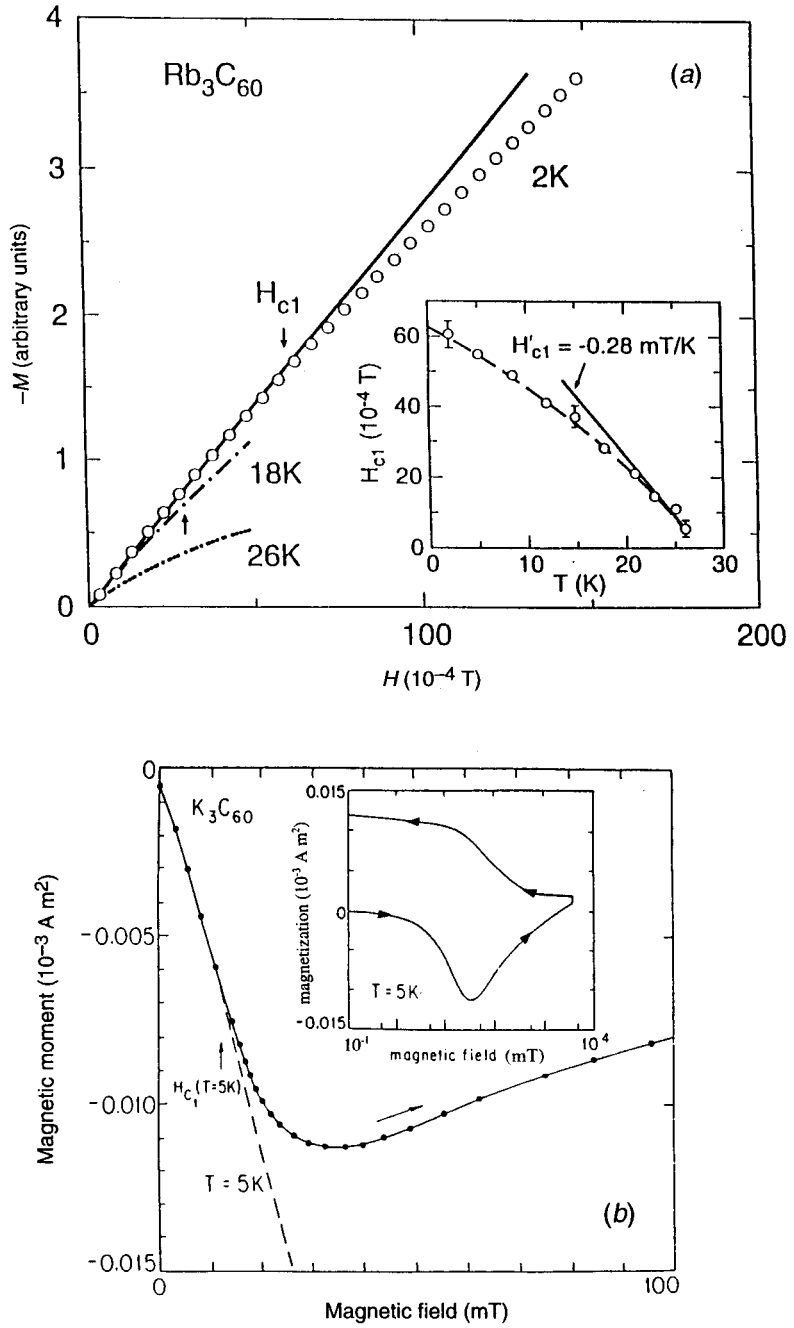

Fig. 20. (*a*) Magnetic field dependence of the magnetisation of polycrystalline Rb_3C_{60} at various temperatures. The inset shows the temperature dependence of H_{c1} [from Ref. 32]. (*b*) Magnetic field dependence of the magnetisation of polycrystalline K_3C_{60} at 5 K [from Ref. 179].

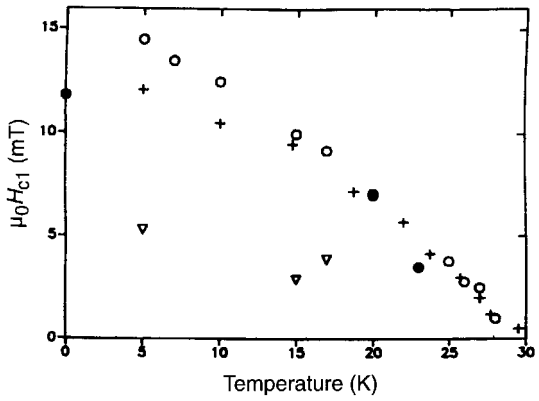

Fig. 21. Lower critical field H_{c1} versus temperature: o, Buntar *et al.* [180]; +, Sparn *et al.* (161); and ●, Politis *et al.* (183). Triangles are the data obtained using Bean's critical state model [204].

We performed such measurements on $RbCs_2C_{60}$ powder and on crystalline Rb_3C_{60} and K_3C_{60} samples [181]. The magnetic field dependence of M_t at $T = 5$ K for a K_3C_{60} single crystal with a shielding fraction of 100% is shown in Fig. 22. Preliminary ac measurements indicate that there is no granularity for current flow in the sample, i.e. there should be no influence of weak links or intergranular boundaries.

As expected, at small fields $H < H_t$ there is no trapped moment, m has some background value and is field independent. When the magnetic field exceeds some characteristic field H_t, a trapped moment appears and increases with increasing external field. The $m_t(H)$ dependence follows ${m_t}^{1/2} \sim H$ as predicted in Ref. [208]. The very unexpected result is that the values of H_t are very small (not higher than 1 mT at zero temperature) in comparison with those values of H_{c1} obtained previously from δM measurements. Such small values of H_t are observed for powders and crystals of different quality. Therefore, it is very unlikely that the trapped moment appears at small fields because of granularity or imperfections of the samples. We can certainly state that the lower critical fields of these fullerenes are not higher than the values of H_t observed in these experiments, because the magnetic field has clearly penetrated the sample (Fig. 22). The temperature dependence of the lower critical field for K_3C_{60} and Rb_3C_{60} crystalline and $RbCs_2C_{60}$ powdered samples obtained by measuring the trapped moment is shown in Fig. 18. We obtain the corresponding values of λ as 890, 850 and 720 nm. The corresponding Ginzburg–Landau parameters for these compounds obtained from our experimental data are $\kappa = 342$, 315 and 163 respectively.

Small values of the field at which the trapped magnetisation appeared, similar to our results, were also observed by Kraus *et al.* [209], who measured the irreversible $M(T)$ curves. Additionally, in several publications small values of the penetration field were obtained [204, 210, 211], but attributed to the breaking of intergranular coupling. Moreover, in more direct measurements of λ [212, 213] by μSR experiments the penetration depth was found to be 480 nm for K_3C_{60} and 420 nm for Rb_3C_{60}, which leads to $\mu_0 H_{c1}(0) = 4{\cdot}0$ and $4{\cdot}9$ mT respectively,

while from optical reflectivity measurements [214] the penetration depth for K_3C_{60} and Rb_3C_{60} was found to be 800 nm. All of these data compel us to undertake more detailed and careful investigations of the lower critical field in fullerenes.

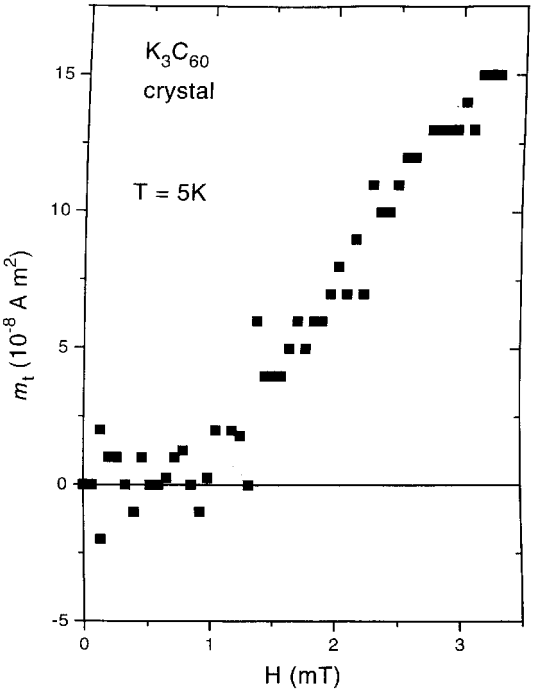

Fig. 22. Magnetic field dependence of the trapped magnetic moment m_t at $T = 5$ K for a K_3C_{60} single crystal. [From Ref. 182]

6. Pinning Problems

As shown in the previous sections, there is good evidence that flux lines penetrate the fullerene superconductors. Because of the three-dimensional structure of the fullerene superconductors, these lines should build up an Abrikosov vortex lattice. As we discussed before, vortices are pinned by pinning centres, i.e. various structural defects in the material. Information on what kind of structural defects act as pinning centres and on the strength of the pinning force produced by these defects is very important from both the fundamental point of view and for the applicability of these materials. However, nothing is known about structural defects in fullerene superconductors by now and, therefore, we do not have any information about the nature of pinning of magnetic flux in these substances. The only point we can make is that pinning in fullerenes is strong, based on the large hysteresis of the $M(H)$ dependence and the large differences between the ZFC and the FC curves. (Experimental data related to flux pinning in fullerene superconductors are summarised in detail in Ref. [215].)

New research has to be performed on samples of good quality with known structural features and structural defects to provide us with this very important information on fullerene superconductors.

7. Conclusions

In the present contribution we discussed some experimental results on structural and magnetic properties of pure fullerenes as well as of some intercalated ones, including those which exhibit superconductivity. All of these compounds show a number of transitions both of the solid state and the magnetic phases. Though many unusual and interesting phenomena have been discovered, many fundamental questions remain unsolved. For instance, why do higher fullerenes not show ferromagnetism (intercalated by TDAE) and superconductivity (intercalated by alkali, alkali-earth or rare-earth metals)? What is the nature of the magnetism in TDAE-C_{60}? What is the mechanism of superconductivity in the fullerenes? Although superconductivity should be related to some kind of electron pairing, details of the pairing mechanism are not well established [34].

There are some further open questions on the superconducting properties of fullerenes. One of them is their instability in air. It is enough to expose the material to air for a fraction of a second to completely destroy superconductivity. We believe that one of the most important goals at the moment is to overcome this barrier.

While the development of sample preparation techniques is very rapid, a well developed procedure to prepare crystalline samples of good quality is still lacking. The lattice of pure C_{60} crystals is usually damaged during doping and a mosaic structure appears. This mosaic structure, in addition to all other structural defects, can strongly affect flux pinning. Moreover, there is almost no information on point defects, vacancies in alkali metal or fullerene sublattices, twin boundaries, etc. in pure C_{60} crystals or in intercalated ones.

The effect of granularity in powdered samples and the possible granularity of bulk crystals [203, 217] represent a central problem at present because one needs to know whether the parameters obtained from experiment are characteristic of the bulk material or of weak links, in order to establish the intrinsic superconducting parameters of these new superconductors. We believe that with the increasing quality of single crystals, significant progress towards a better understanding of the mixed state properties lies immediately ahead, and that magnetisation measurements and their comparison with other techniques will play a key role in this development.

In addition, it will be worth while to search for superconductivity in the polymeric AC_{60} compounds, for instance in KC_{60}, which remains metallic down to very low temperatures.

Acknowledgments

The authors are grateful to Professors J. E. Fischer, H. Kuzmany and M. Ricco and to Drs G. Sparn, M. Kraus, M. Baenitz and J. A. Henderson for numerous helpful discussions and assistance, and to their colleagues from the Low Temperature Laboratory, Atominstitut, for help with the experiments. This work is supported by the Fonds zur Förderung der Wissenschaftlichen Forschung, Wien, under project P11177-PHY and partly under project M00116-PHY.

References

[1] Rohlfing, E. A., Cox, D. M., and Kaldor, A. (1984). J. Chem. Phys. **81**, 3322.
[2] Kroto, H. W., Heath, J. R., O'Brien, S. C., Curl, R. F., and Smalley, R. E. (1985). Nature **318**, 162.

[3] Krätschmer, W., Lamb, L. D., Fostiropoulos, K., and Huffman, D. R. (1990). Nature **347**, 345.
[4] Special issue on fullerenes. (1992). Accounts of Chemical Research **25**.
[5] Special issue on fullerenes. (1992). Carbon **8**, Number 8.
[6] Special issue on fullerenes. (1992). J. Phys. Chem. Solids **53**, Number 12.
[7] Special issue on fullerenes. (1993). J. Phys. Chem. Solids **54**, Number 12.
[8] Special issue on fullerenes. (1994). MRS Bulletin XIX, Number 11.
[9] Weltner, W., Jr, and Van Zee, R. J. (1989). Chem. Rev. **89**, 1713.
[10] Averback, R. S., Bernholz, J., and Nelson, D. L. (Eds) (1991). 'Clusters and Cluster-assembled Materials', MRS Sympos. Ser., Vol. 206 (Material Research Society: Boston).
[11] Curl, R. F., and Smalley, R. E. (1991). Scient. Am., October, p. 32.
[12] Kroto, H. W., Allaf, A. W., and Balm, S. P. (1991). Chem. Rev. **91**, 1213.
[13] Hammond, G. S., and Kuck, V. J. (Eds) (1992). 'Fullerenes', ACS Sympos. Ser., Vol. 481 (Am. Chem. Society: Washington DC).
[14] Taliani, C., Ruani, G., and Zamboni, R. (Eds) (1992). 'Fullerenes: Status and Perspectives' (World Scientific: Singapore).
[15] Renschler, C. L., Pouch, J. J., and Cox, D. M. (Eds) (1992). 'Novel Forms of Carbon', MRS Symp. Ser., Vol. 170 (Material Research Society: San Francisco).
[16] Diederich, F., and Rubin, Y. (1992). Angew. Chem. Int. Ed. Engl. **31**, 1101.
[17] Hebard, A. F. (1992). Phys. Today **45**, 26.
[18] Kroto, H. W., Fischer, J. E., and Coy, D. E. (Eds) (1993). 'The Fullerenes' (Pergamon: Oxford).
[19] Kumar, V., Martin, T. P., and Tosatti, E. (Eds) (1993). 'Clusters and Fullerenes' (World Scientific: Singapore).
[20] Stephens, P. W. (Ed.) (1993). 'Physics and Chemistry of Fullerenes' (World Scientific: Singapore).
[21] Kuzmany, H., Fink, J., Mehring, M., and Roth, G. (Eds) (1993). 'Electronic Properties of Fullerenes', Springer Series in Solid State Science, Vol. 117 (Springer: Berlin).
[22] Billups, W. E., and Ciufolini, M. A. (Eds) (1993). 'Buckminsterfullerenes' (Springer: Berlin).
[23] Hebard, A. F. (1993). Ann. Rev. Mat. Sci. **23**, 159.
[24] Meingast, C., and Gugenberger, F. (1993). Mod. Phys. Lett. **B7**, 1703.
[25] Ogata, H., et al. (1993). Mod. Phys. Lett. **B7**, 1173.
[26] Hirsh, A. (1993). 'The Chemistry of Fullerenes' (Thieme: Berlin).
[27] Prassides, K. (Ed.) (1994). 'Physics and Chemistry of Fullerenes' (Kluwer: Dordrecht).
[28] Kuzmany, H., Fink, J., Mehring, M., and Roth, G. (Eds) (1994). 'Progress in Fullerene Research' (World Scientific: Singapore).
[29] Kadish, K. M., and Ruoff, R. S. (Eds) (1994). 'Recent Advances in the Chemistry and Physics of Fullerenes and Related Materials I' (ECS Proc. Ser.: Pennington, NJ).
[30] Baggot, J. (1994). 'Perfect Symmetry: The Accidental Discovery of a New Form of Carbon' (Oxford Univ. Press).
[31] Weaver, J. H., and Poirier, D. M. (1994). 'Solid State Physics' 48 (Eds H. Ehrenreich and F. S. Paepen) (Academic: New York).
[32] Ramirez, A. P. (1994). Superconduct. Rev. **1**, 1.
[33] Gelfand, M. P. (1994). Superconduct. Rev. **1**, 103.
[34] Dresselhaus, M. S., Dresselhaus, G., and Saito, S. (1994). In 'Physical Properties of High Temperature Superconductors IV' (Ed. D. M. Ginsberg) (World Scientific: Singapore).
[35] Kuzmany, H., Fink, J., Mehring, M., and Roth, G. (Eds) (1995). 'Physics and Chemistry of Fullerenes and Derivatives' (World Scientific: Singapore).
[36] Kadish, K. M., and Ruoff, R. S. (Eds) (1995). 'Recent Advances in the Chemistry and Physics of Fullerenes and Related Materials II' (ECS Proc. Ser.: Pennington, NJ).
[37] Kadish, K. M., and Ruoff, R. S. (Eds) (1996). 'Recent Advances in the Chemistry and Physics of Fullerenes and Related Materials II' (ECS Proc. Ser.: Pennington, NJ).
[38] Buntar, V., and Weber, H. W. (1996). Physica Nizkih Temperatur **22**, 231.
[39] Elser, V., and Haddon, R. C. (1987). Nature **325**, 792.
[40] Elser, V., and Haddon, R. C. (1987). Phys. Rev. **A36**, 4579.

[41] Haddon, R. C., et al. (1991). Nature **350**, 46.
[42] Ruoff, R. S., et al. (1991). J. Phys. Chem. **95**, 46.
[43] Pasquarello, A., Schlueter, M., and Haddon, R. C. (1992). Science **257**, 1660.
[44] Pasquarello, A., Schlueter, M., and Haddon, R. C. (1993). Phys. Rev. **A47**, 1783.
[45] Haddon, R. C., and Pasquarello, A. (1994). Phys. Rev. **B50**, 16459.
[46] Ramirez, A. P., et al. (1994). Science **265**, 84.
[47] Hamada, N., Sawada, S., and Oshijama, A. (1992). Phys. Rev. Lett. **68**, 1579.
[48] Byszewski, P., and Baran, M. (1995). Europhys. Lett. **31**, 363.
[49] Sachidanadan, R. A., and Harris, A. B. (1991). Phys. Rev. Lett. **67**, 1467.
[50] de Bruijn, J., et al. (1993). Europhys. Lett. **24**, 551.
[51] Fleming, R. M., et al. (1991). In 'Clusters and Cluster-assembled Materials' (Eds S. Averback et al.), MRS Symp. Proc. 206 (Materials Research Society: Boston).
[52] Heiney, P. A., Fischer, J. E., McGhie, A. R., Romanow, W. J., Denenstein, A. M., McCauley, J. P., and Smith III, A. B. (1991). Phys. Rev. Lett. **66**, 2911.
[53] Dworkin, A., et al. (1991). Comp. Rendu. Acad. Sci., Paris-Serie II, **312**, 979.
[54] David, W. I. F., Ibberson, R. M., Dennis, T. J. S., Hare, J. P., and Prassides, K. (1992). Europhys. Lett. **18**, 219.
[55] Yu, R. C., Tea, N., Salamon, M. B., Lorentz, D., and Malhotra, R. (1992). Phys. Rev. Lett. **68**, 2050.
[56] Lu, J. P., Li, X. P., and Martin, R. M. (1992). Phys. Rev. Lett. **68**, 1551.
[57] Shi, X. D., Kortan, A. R., Williams, J. M., Kini, A. M., Savall, B. M., and Chaikin, P. M. (1992). Phys. Rev. Lett. **68**, 827.
[58] Alers, G. B., et al. (1992). Science **257**, 511.
[59] Gugenberger, F., et al. (1992). Phys. Rev. Lett. **69**, 3774.
[60] Grivei, E., Nysten, B., Cassart, M., et al. (1993). Phys. Rev. **B47**, 1705.
[61] Matsuo, T., et al. (1992). Solid State Commun. **83**, 711.
[62] Buntar, V., Weber, H. W., and Ricco, M. (1995). Solid State Commun. **98**, 175.
[63] Song, L. W., et al. (1993). Solid State Commun. **87**, 387.
[64] Gigoryan, L., and Tokumoto, M. (1995). Solid State Commun. **96**, 523.
[65] Grushko, Yu., private communication.
[66] Li, X. P., Lu, J. P., and Martin, R. M. (1992). Phys. Rev. **B46**, 4301.
[67] Burgos, E., Halas, E., and Bonadeo, H. (1993). Phys. Rev. **B47**, 7542.
[68] Zubov, V. I., Tretiakov, N. P., Sanches, J. F., and Caparica, A. A. (1996). Phys. Rev. **B53**, 12080.
[69] Vaughan, G. B. M., et al. (1991). Science **254**, 1350.
[70] Fleming, R. M., et al. (1991). Phys. Rev. **B44**, 888.
[71] Verheijen, M. A., et al. (1992). Chem. Phys. **166**, 287.
[72] Tendeloo, G. V., et al. (1993). Europhys. Lett. **21**, 329.
[73] Mitsuki, T., et al. (1994). Jpn J. Appl. Phys. **33**, 6281.
[74] Tomita, M., et al. (1992). Appl. Phys. Lett. **61**, 1171.
[75] Oh, D. H., and Lee, Y. H. (1995). Phys. Rev. Lett. **75**, 4230.
[76] Christides, C., et al. (1993). Europhys. Lett. **22**, 611.
[77] Maniva, Y., et al. (1993). J. Phys. Soc. Jpn **62**, 1131.
[78] Tycko, R., et al. (1993). Chem. Phys. **99**, 7554.
[79] Blink, R., Dolinsek, J, Seliger, J., and Arcon, D. (1993). Solid State Commun. **88**, 9.
[80] Prassides, K., et al. (1992). J. Phys. Chem. **96**, 10600.
[81] Dennis, T. J. S., et al. (1993). J. Phys. Chem. **97**, 8553.
[82] Christides, C., et al. (1994). Phys. Rev. **B49**, 2897.
[83] Renker, B., et al. (1993). Z. Phys. **B90**, 325.
[84] Tomanek, D., et al. (1993). J. Phys. Chem. Solids **54**, 1679.
[85] Heath, J. R., et al. (1985). J. Am. Chem. Soc. **107**, 779.
[86] Johnson, R. D., et al. (1992). Nature **355**, 239.
[87] Johnson, R. D., Bethune, D. S., and Yannoni, C. S. (1992). Acc. Chem. Res. **25**, 169.
[88] Bandow, S., et al. (1993). J. Phys. Chem. **97**, 6101.
[89] Yannoni, C. S., et al. (1993). Synthetic Metals **59**, 279.
[90] Benthune, D. S., et al. (1992). Nature **366**, 123.
[91] Kato, T., et al. (1993). J. Phys. Chem. **97**, 13425.

[92] Hoinkis, M., et al. (1992). Chem. Phys. Lett. **198**, 461.
[93] Allemand, P., et al. (1991). Science **253**, 301.
[94] Li, Y., et al. (1993). Solid State Commun. **86**, 475.
[95] Stephens, P. W., et al. (1992). Nature **355**, 331.
[96] Schlider, A., et al. (1994). Phys. Rev. Lett. **73**, 1299.
[97] Hassanien, A., et al. (1995). p. 498 in Ref. [35].
[98] Arovas, D. P., and Auerbach, A. (1995). Phys. Rev. **B52**, 10114.
[99] Tanaka, K., et al. (1993). Phys. Rev. **B47**, 7554.
[100] Susuki, A., et al. (1994). Chem. Phys. Lett. **223**, 517.
[101] Tanaka, K., et al. (1995). Chem. Phys. Lett. **237**, 123.
[102] Tanaka, K., et al. (1994). Chem. Phys. Lett. **230**, 271.
[103] Venturini, P., et al. (1992). Int. J. Mod. Phys. **6**, 3947.
[104] Cristofolini, L., et al. (1994). p. 279 in Ref. [28].
[105] Lappas, A., et al. (1995). Science **267**, 1799.
[106] Ricco, M., et al. (1995). p. 500 in Ref. [35].
[107] Blinc, R., et al. (1996). Phys. Rev. Lett. **76**, 523.
[108] Dzyaloshinsky, I. (1958). J. Phys. Chem. Solids **4**, 241.
[109] Moriya, T. (1960). Phys. Rev. Lett. **4**, 228.
[110] Michailovic, D., et al. (1995). Science **268**, 400.
[111] Tanaka, K., et al. (1992). Phys. Lett. **A164**, 221.
[112] Tanaka, K., et al. (1993). Solid State Commun. **85**, 69.
[113] Bommeli, F., et al. (1995). Phys. Rev. **B51**, 1366.
[114] Winter, J., and Kuzmany, H. (1992). Solid State Commun. **84**, 935.
[115] Zhu, Q., et al. (1993). Phys. Rev. **B47**, 13948.
[116] Tycko, T., et al. (1993). Phys. Rev. **B48**, 9097.
[117] Chauvet, O., et al. (1994). Phys. Rev. Lett. **72**, 2721.
[118] Pekket, S., et al. (1994). Solid State Commun. **90**, 349.
[119] Stephens, P. W., et al. (1994). Nature **370**, 636.
[120] Pekket, S., et al. (1994). Science **265**, 1077.
[121] Rao, A. M., et al. (1993). Science **259**, 955.
[122] Robert, J., et al. (1995). Solid State Commun. **96**, 143.
[123] Erwin, S. C., Krishna, G. V., and Mele, E. J. (1995). Phys. Rev. **B51**, 7345.
[124] Mele, E. J., Krishna, G. V., and Erwin, S. C. (1995). Phys. Rev. **B52**, 12493.
[125] Uemura, Y., et al. (1995). Phys. Rev. **B52**, R6991.
[126] MacFarlane, W., et al. (1995). Phys. Rev. **B52**, R6995.
[127] Cristofolini, L., et al. (1995). J. Phys. Cond. Matter **7**, L567.
[128] Hariyaga, K. (1996). Phys. Rev. **B53**, R4197.
[129] Bommeli, F., et al. (1995). Phys. Rev. **B51**, 20.
[130] Janossy, A., et al. (1993). Phys. Rev. Lett. **71**, 1091.
[131] Martin, M. C., et al. (1995). Phys. Rev. **B51**, 3210.
[132] Zhu, Q., Cox, D. E., and Fischer, J. E. (1995). Phys. Rev. **B51**, 3966.
[133] Oszlany, G., et al. (1995). Phys. Rev. **B51** 12228.
[134] Granasy, L., et al. (1996). Solid State Commun. **97**, 573.
[135] Kosaka, M., et al. (1995). Phys. Rev. **B51**, 12018.
[136] Lappas, A., et al. (1995). J. Am. Chem. Soc. **117**, 7560.
[137] Hannay, N. B., et al. (1965). Phys. Rev. Lett. **14**, 225.
[138] Hadon, R. C., et al. (1991). Nature **350**, 320.
[139] Hebard, A. F., et al. (1991). Nature **350**, 600.
[140] Rosseinsky, M. J.,, et al. (1991). Phys. Rev. Lett. **66**, 2830.
[141] Bednorz, J. G., and Müller, K. A. (1986). Z. Phys. **B64**, 189.
[142] Chu, C. W., et al. (1987). Phys. Rev. Lett. **58**, 405.
[143] Tanigaki, K., et al. (1992). Nature **356**, 419.
[144] Palstra, T. T. M., et al. (1995). Solid State Commun. **93**, 327.
[145] Tanigaki, K., et al. (1993). J. Phys. Chem. Solids **54**, 1645.
[146] Stephens, P. W., et al. (1991). Nature **351**, 632.
[147] Kortan, A. R., et al. (1992). Nature **355**, 529.
[148] Kortan, A. R., et al. (1992). Nature **360**, 566.

[149] Kraus, M., et al. (1995). Fullerene Sci. & Tech. **3**, 115.
[150] Kortan, A. R., Kopylov, N., and Özdas, E., in Ref. [37].
[151] Yamanaka, S., in Ref. [29].
[152] Tanigaki, K., Zhou, O., Kuroshima, S., Ibid.
[153] Saito, S., Ibid.
[154] Saito, S., Buntar, V., Ibid.
[155] Fleming, R. M., et al. (1991). Nature **352**, 787.
[156] Zhou, O., et al. (1992). Science **255**, 833.
[157] Oshiyama, A., and Saito, S. (1992). Solid State Commun. **82**, 41.
[158] Ramirez, A. P., Rosseinsky, M. J., Murphy, D. W., and Haddon, R. C. (1992). Phys. Rev. Lett. **69**, 1687.
[159] Tyco, R., et al. (1991). Science **253**, 884.
[160] Schirber, J. E., et al. (1991). Physica **C178**, 137.
[161] Sparn, G., et al. (1992). Phys. Rev. Lett. **68**, 1228.
[162] Schirber, J. E., et al. (1993). J. Phys. Chem. Sol. **54**, 1427.
[163] Kniaz, K., et al. (1993). Solid State Commun. **88**, 47.
[164] Prassides, K., et al. (1994). Science **263**, 950.
[165] Yildirim, T., Fischer, J. E., Dinnebier, R., Stephens, P. W., and Lin, C. L. (1995). Solid State Commun. **93**, 269.
[166] Yildirim, T., et al. (1993). Phys. Rev. Lett. **71**, 1383.
[167] Kochanski, G. P., Hebard, A. F., Haddon, R. C., and Fiory, A. T. (1992). Science **255**, 184.
[168] Stepniak, F., et al. (1993). Phys. Rev. **B48**, 1899.
[169] Xiang, X.-D., et al. (1992). Science **256**, 1190.
[170] Hebard, A. F., Palstra, T. T. M., Haddon, R. C., and Fleming, R. M. (1993). Phys. Rev. **B48**, 9945.
[171] Vareka, W. A., Fuhrer, M. S., and Zettl, A. (1994). Physica **C235–40**, 2507.
[172] Wong, W. H., et al. (1992). Europhys. Lett. **18**, 79.
[173] Hou, J. G., et al. (1995). Solid State Commun. **93**, 973.
[174] Lee, M. W., et al. (1995). Physica **C245**, 6.
[175] Ogata, H., et al. (1992). Jpn J. Appl. Phys. **31**, L166.
[176] Palstra, T. T. M., et al. (1992). Phys. Rev. Lett. **68**, 1054.
[177] Quirion, G., et al. (1993). Europhys. Lett. **21**, 233.
[178] Yan, D., and Li, W. (1995). Phys. Lett. **A208**, 335.
[179] Holczer, K., et al. (1991). Phys. Rev. Lett. **67**, 271.
[180] Politis, C., Buntar, V., Krauss, W., and Gurevich, A. (1992). Europhys. Lett. **17**, 175.
[181] Buntar, V., Sauerzopf, F. M., and Weber, H. W. (1996). Phys. Rev. **B54**, R9651.
[182] Buntar, V., Sauerzopf, F. M., Weber, H. W., Fischer, J. E., Kuzmany, H., Halushka, M., and Lin, C. L. (1996). Phys. Rev. **B54**, 14952.
[183] Politis, C., Sokolov, A. I., and Buntar, V. (1992). Mod. Phys. Lett. **B6**, 351.
[184] Buntar, V., Ricco, M., Cristofolini, L., Weber, H. W., and Bolzoni, F. (1995). Phys. Rev. **B52**, 4432.
[185] Khairullin, I. I., Imaeda, K., Yakushi, K., and Inokuchi, H. (1994). Physica C **231**, 26.
[186] Stenger, V. A., Pennington, C. H., Buffinger, D. R., and Ziebarth, R. P. (1995). Nuclear magnetic resonance of A_3C_{60} superconductors, preprint.
[187] Tokumoto, M., et al. (1993). Phys. Chem. Sol. **54**, 1667.
[188] Imaeda, K., Khairullin, I. I., Yakushi, K., and Inokuchi, H. (1997). Proc. ICSM'94 (Seoul), Synth. Metals, in press.
[189] Sokolov, A. I., Kufaev, Yu. A., and Sonin, E. B. (1993). Physica **C212**, 19.
[190] Baenitz, M., et al. (1994). Physica **C228**, 181.
[191] Hou, J. G., et al. (1993). Solid State Commun. **86**, 643.
[192] Hou, J. G., et al. (1994). Physica **C228**, 175.
[193] Gu, C., et al. (1994). Phys. Rev. **B50**, 16566.
[194] Johnson, C. E., et al. (1992). Phys. Rev. **B46**, 5880.
[195] Boebinger, G. S., et al. (1992). Phys. Rev. **B46**, 5876.
[196] Foner, S., et al. (1992). Phys. Rev. **B46**, 14936.
[197] Hou, J. G., et al. (1994). Physica **C232**, 22.

[198] Politis, C., Buntar, V., and Seminozhenko, V. P. (1993). Int. J. Mod. Phys. **B7**, 2163.
[199] Baenitz, M., et al. (1995). p. 436 in Ref. [35].
[200] Korenivski, V. V., Rao, K., and Iqbal, Z. (1994). Phys. Rev. **B50**, 13890.
[201] Werthamer, N. R., Helfand, E., and Hohenberg, P. C. (1966). Phys. Rev. **147**, 295.
[202] de Gennes, P. G. (1966). 'Superconductivity of Metals and Alloys' (W. A. Benjamin: New York).
[203] Buntar, V., Sauerzopf, F. M., Weber, H. W., Fischer, J. E., Kuzmany, H., Halushka, M., and Lin, C. L., in Ref. [37].
[204] Buntar, V., Eckern, U., and Politis, C. (1992). Mod. Phys. Lett. **B6**, 1037.
[205] Bean, C. P. (1962). Phys. Rev. Lett. **8**, 250.
[206] Abrikosov, A. A. (1957). Zh. Eksp. Teor. Fiz, **32**, 1442.
[207] Böhmer, C. (1995). The lower critical field in high-T_c single crystals, Ph.D. Thesis, Technical University, Vienna, unpublished.
[208] Moshchalkov, V., et al. (1991). Physica **C175**, 407.
[209] Kraus, M., et al. (1996). J. Phys. Chem. Solids **57**, 999.
[210] Thompson, J. D., et al. (1994). In 'Physical and Material Properties of High Temperature Superconductors' (Eds S. K. Malic and S. S. Shah), p 139 (Nova Science: Commack, NJ).
[211] Irons, S. H., Liu, J. Z., Klavins, P., and Shelton, R. N. (1995). Phys. Rev. **B52**, 15517.
[212] Uemura, Y. J., et al. (1991). Nature **352**, 606.
[213] Uemura, Y. J., et al. (1994). Physica **C235–40**, 2501.
[214] Degiorgi, L., et al. (1992). Phys. Rev. Lett. **69**, 2987.
[215] Buntar, V., and Weber, H. W. (1996). Supercond. Sci. & Techn. **9**, 1.
[216] Lin, C. L., et al. (1994). Solid State Commun. **90**, 629.
[217] Buntar, V., et al., to be published.
[218] Tycko, R., et al. (1992). Phys. Rev. Lett. **68**, 1912.
[219] Degiorgi, L., et al. (1992). Phys. Rev. Lett. **69**, 2987.
[220] Lin, C. L., et al. (1994). Phys. Rev. **B49**, 4285.
[221] Heinze, M., et al. (1996). Synthetic Metals **77**, 23.
[222] Sakamoto, N., et al. (1995). Jap. J. Appl. Phys. **34**, L1267.
[223] Lee, M. W., et al. (1995). Jap. J. Appl. Phys. **34**, 126.
[224] Tycko, R., et al. (1992). Phys. Rev. Lett. **68**, 1912.
[225] Gupta, R. P. (1994) Physica **C235–40**, 2497.
[226] Els, G., et al. (1994). Physica **C235–40**, 2475.
[227] Jess, P., et al. (1994). Physica **C235–40**, 2499.
[228] Abrefah, J., Olander, D. R., Balooch, M., and Siekhaus, W. J. (1992). Appl. Phys. Lett. **59**, 3402.
[229] Tokmakoff, A., Haynes, D. R., and George, S. M. (1991). Chem. Phys. Lett. **186**, 450.
[230] Fischer, J. E., et al. (1991). Science **352**, 1288.
[231] Duclos, S. J., et al. (1991). Nature **351**, 380.
[232] Li, J., et al. (1992). Physica **C195**, 205.
[233] Heiney, P. A., et al. (1992). Phys. Rev. **B45**, 4544.
[234] Beyermann, W. P., et al. (1992). Phys. Rev. Lett. **68**, 2046.
[235] Ren, S. L., et al. (1991). Appl. Phys. Lett. **59**, 2678.
[236] Hebard, A. F., et al. (1991). Appl. Phys. Lett. **59**, 2678.
[237] Hansen, P. L., Fallon, P. J., and Krätschmer, W. (1991). Chem. Phys. Lett. **181**, 367.
[238] Skumanich, A. (1991). Chem. Phys. Lett. **182**, 486.
[239] Reber, C., et al. (1991). J. Chem. **95**, 2127.
[240] Gensterblum, G., et al. (1991). Phys. Rev. Lett. **67**, 2171.
[241] Mort, J., et al. (1991). Chem. Phys. Lett. **186**, 284.
[242] David, W. I. F., et al. (1991). Nature **353**, 147.
[243] Yang, S. H., et al. (1987). Chem. Phys. Lett. **139**, 233.
[244] Lichtenberger, D. L., et al. (1991). Chem. Phys. Lett. **176**, 203.
[245] Tomanek, D., Schluter, M. A. (1991). Phys. Rev. Lett. **67**, 2331.
[246] Hettich, R. L., et al. (1991). Phys. Rev. Lett. **67**, 1242.
[247] Ugarte, D. (1993). Chem. Phys. Lett. **207**, 473.
[248] Osawa, E., et al. (1994). p. 33 in Ref. [8].

[249] Sparn, G., et al. (1992). Solid State Commun. **82**, 779.
[250] Murphy, D. W., et al. (1992). J. Phys. Chem. Sol. **53**, 1321.
[251] Mizuki, J., et al. (1994). Phys. Rev. **B50**, 3466.

Manuscript received 22 July, accepted 4 October 1996